Westfälische Wilhelms-Universität Münster

Bachelor-thesis

Lukas Bremer (Email: l_brem04@uni-muenster.de)

Direct Photon Production in Proton-Proton-Collisions

First examiner: PD Dr. Karol Kovařik
Second examiner: Prof. Dr. Michael Klasen

15.09.2021

Direct Photon Production in Proton-Proton-Collisions

Lukas Bremer

Abstract

A description of the internal structure of protons is usually complex and accompanied by qumbersome calculations. Direct photon production can therefore give a comparatively simple *insight* into *proton structure* described by *QCD*.
For this purpuse, the *WA70 collaboration* made experiments on hadron-hadron collisions at the *CERN SPS* from 1984 to 1986. Here made experiments comprised proton-proton- and proton-pion-collisions and measured prompt photon production. In order to describe these experiments at tree level, the following subprocesses must be considered

1. $qg \to q\gamma$ hard compton scattering
2. $\bar{q}g \to \bar{q}\gamma$ anti compton scattering
3. $q\bar{q} \to g\gamma$ quark-antiquark annihilation.

The aim of this thesis is to describe the direct photon production at *tree level* and to investigate the reliability of the leading order calculation, by comparison with results from the *WA70 collaboration*. Furthermore, the ratios of the contributing processes are to be computed.
For this purpose, we will have a glimpse on how couplings in *QED* and *QCD* are to be calculated, based on *gauge transformations* in section 1. To describe hard processes in hadronic collisions the strong coupling constant and *PDFs* are described in section 2 and section 3. The following sections (section 4 to section 7) are used for the calculation of the differential cross-section by evaluating the *matrix elements* and describing the *kinematics* of the system. Subsequently, we will compare the results with the measurements of the *WA70 collaboration* and evaluate them against this background.

Contents

1 Gauge Transformations

In 1788, the Italian-French mathematician Joseph-Louis Lagrange reformulated classical mechanics in the Lagrange formalism. The foundation is the principle of least action. This states that nature always minimizes the action S on a given trajectory. Based on this principle, the Lagrange-equations of motion can be derived, which describe the system's dynamics.
We can apply the Lagrange-formalism to quantum systems as well. However, considering that we have to describe particles in quantum mechanics as waves or fields, the Lagrangian for point-like particles is no longer adequate. Fields have no well-defined location x in space-time, similar to a fluid. So the Lagrangian has to be written as a density $\mathscr{L}$

$$\mathcal{L} = \int \mathscr{L} d^3x \tag{1.1}$$

$$S = \int \mathcal{L} dt = \int \mathscr{L} d^4x. \tag{1.2}$$

As mentioned before, the Lagrangian provides us with the most fundamental information of our system. Therefore, it is the centerpiece of quantum field theory. From here on, all further steps like Feynman rules are developed. Similarly, properties of our systems can be deduced from the Lagrangian as well. Quantum field theory describes interactions of particles as the coupling of fields. To receive the Lagrangians for the electromagnetic- and strong-force, we are going to look at symmetries, or more precisely gauge symmetries. A gauge describes a change of parameters that does not affect physics. In the next section, the Lagrangians for QED and QCD are developed by demanding a certain gauge invariance.

1.1 U(1) Transformations

To derive Lagrangians for interaction of particles, we require the Lagrangians for free particles. Those are given by $\mathscr{L}_{Dirac}$ for free spinor fields ψ and $\mathscr{L}_{Maxwell}$ for massless vector fields A

$$\mathscr{L}_{\text{Dirac}} = \hat{\psi}\left(i\gamma_\mu \partial^\mu - m\right)\psi \tag{1.3}$$

$$\mathscr{L}_{\text{Maxwell}} = \frac{1}{2} F^{\mu\nu} F_{\mu\nu} = \frac{1}{2}\left(\partial^\mu A^\nu \partial_\mu A_\nu - \partial^\mu A^\nu \partial_\nu A_\mu\right). \tag{1.4}$$

Since information can not travel faster than light, the gauge can not apply globally. Hence, the only physical correct gauge transformation is local, i.e. it has to depend on x. Transforming the spinor field under a local U1 transformation yields [1]

$$\psi \to \psi' = e^{iga(x)}\psi. \tag{1.5}$$

Inserting this into (1.3) leads to an additional term in the Lagrangian. Consequently, the Lagrangian is not gauge invariant

$$\mathscr{L}_{\text{add}} = -\hat{\psi}\gamma_\mu g \partial^\mu a(x)\psi. \tag{1.6}$$

[1] $a(x)$ denotes the group parameter and g an abitrary constant, which we will call charge.

To finally receive gauge invariance under U(1) transformations, we can simply add a new term

$$\mathscr{L}_{\text{gauge}} = \hat{\psi}\gamma_\mu A^\mu \psi. \tag{1.7}$$

This gauge term includes the so-called gauge field A^μ. $\mathscr{L}_{Dirac}$ describes the interaction of two spin-1/2-particles via electromagnetic force, which is mediated by the gauge field (photon field). Under the restriction to get a gauge invariant Lagrangian, the field has to transform as

$$A^\mu \to A'^\mu = A^\mu + \partial^\mu a(x). \tag{1.8}$$

Fortunately, the Maxwell-term is gauge invariant under (1.8), thus the calculation is complete. For a complete description we add up all terms. The covariant derivative includes the additional interaction term D^μ. It is convention, so the Lagrangian has the same form as (1.3). This leads to the Lagrangian of QED

$$\mathscr{L}_{\text{QED}} = \hat{\psi}\left(i\gamma_\mu D^\mu - m\right)\psi + \frac{1}{2}\left(\partial^\mu A^\nu \partial_\mu A_\nu - \partial^\mu A^\nu \partial_\nu A_\mu\right) \tag{1.9}$$

$$D^\mu = \partial^\mu + igA^\mu. \tag{1.10}$$

To summarize, just by starting with the Lagrangians for free fields and applying local gauge symmetry under U(1) transformations, it is possible to derive the interaction Lagrangian for QED. These interactions include charge, which gives the strength of the interaction.[2] We can proceed similarly for SU(3) transformations.

1.2 SU(3) Transformations

A local SU(3) transformation has the form

$$U(x) = e^{ig\alpha_a(x)T_a}. \tag{1.11}$$

Where g stands for an arbitrary constant, which we identify as the coupling constant. In contrast to U(1), the SU(3) has 8 generators T_a, i.e. the index a, so called color index, takes values from 1 to 8. To get a local gauge invariant Lagrangian, we apply a similar step as in (1.10). Again, the index a occurs in (1.12). Because of this, we obtain not one but 8 different gauge fields that have to be considered

$$D^\mu = \partial^\mu + igA_a^\mu T_a. \tag{1.12}$$

Once more, because of SU(3) properties, we have to deal with 3 fermion fields and so QCD differs from QED. The SU(3) generators can be represented as 3×3 matrices, which require three component objects to act on. Having in mind our ansatz (1.12), there have to be 3 fermion fields. To rewrite the Dirac equation, it is helpful to set up the following notation

$$\bar{u} = \begin{pmatrix}\psi_1, & \psi_2, & \psi_3\end{pmatrix} \qquad u = \begin{pmatrix}\psi_1 \\ \psi_2 \\ \psi_3\end{pmatrix}. \tag{1.13}$$

[2] Furthermore, the Noether Theorem for field theories, leads to the conservation of electrical charge.

These objects have dirac spinors as components and transform under local SU(3) transformation as

$$u' = U(x)u \qquad \bar{u}' = \bar{u}U^\dagger(x). \tag{1.14}$$

Obviously, the assumption of quarks with equal masses makes the part of $\mathscr{L}_{Dirac}$ that includes m gauge invariant, because the mass term in reads $m\,\mathbb{1}$. Writing the non-trivial part of the Dirac equation in 3 components yields

$$\mathscr{L}_{Dirac} = i\bar{u}\gamma_\mu D^\mu u. \tag{1.15}$$

The intention is to make this Lagrangian gauge invariant under SU(3) transformation. We can achieve a local transformation by inserting (1.14) into (1.15) and transforming the covariant derivative. Clearly the following ansatz for the transformation behaviour of D^μ achieves our goal [3]

$$D'^\mu \stackrel{!}{=} U(x)D^\mu U^\dagger(x). \tag{1.16}$$

Under the assumption that the covariant derivative transforms as (1.16), it is possible to determine the Maxwell term in the next step. Therefore, the following notations are usefull

$$\mathscr{L}_{Maxwell} = F^{\mu\nu}_a F^a_{\mu\nu} = \mathrm{TR}\left(\mathcal{F}^{\mu\nu}\mathcal{F}_{\mu\nu}\right) \qquad \mathcal{F}_{\mu\nu} = T^a F^a_{\mu\nu} \quad \text{and} \quad \mathcal{A}^\mu = T^a A^a_\mu. \tag{1.17}$$

Unlike in the previous section, $\mathscr{L}_{\mathscr{M}}$ is not gauge invariant anymore. According to the trace theorems, a trace is invariant to cyclic rotations. So in order to receive a gauge invariant maxwell term (1.17), we can simply demand that the field strength tensor $\mathcal{F}^{\mu\nu}$ transforms like

$$\mathcal{F}'^{\mu\nu} \stackrel{!}{=} U(x)\mathcal{F}^{\mu\nu}U^\dagger(x). \tag{1.18}$$

This is the same transformation behaviour as from the covariant derivative D^μ. However, the field strength tensor has two indices and thus the following ansatz fulfills the requirements

$$\mathcal{F}^{\mu\nu} = D^\mu D^\nu = \partial^\mu\partial^\nu + ig\left[\partial^\mu(\mathcal{A}^\nu) + \mathcal{A}^\nu\partial^\mu + \mathcal{A}^\mu\partial^\nu\right] - g^2\mathcal{A}^\nu\mathcal{A}^\mu. \tag{1.19}$$

Due to (1.16) the product $D^\mu D^\nu$ transforms in the same way as D^μ. To get $\mathcal{F}^{\mu\nu}$ into a similar form as from quantum electrodynamics, we can simply substract $D^\nu D^\mu$

$$\mathcal{F}^{\mu\nu} = D^\mu D^\nu - D^\nu D^\mu = ig\left(\partial^\nu\mathcal{A}^\mu - \partial^\nu\mathcal{A}^\mu\right) - g^2\left[\mathcal{A}^\nu, \mathcal{A}^\mu\right]. \tag{1.20}$$

From here on, all further changes do not affect the physical properties of the Lagrangian. It is conventional to divide (1.20) by the factor ig and to add the maxwell term as follows

$$\begin{aligned} \mathscr{L}_{QCD} &= \bar{u}i\gamma_\mu D^\mu u - \frac{1}{4}\mathrm{TR}\left(\mathcal{F}^{\mu\nu}\mathcal{F}_{\mu\nu}\right) \\ \mathcal{F}^{\mu\nu} &= \left(\partial^\nu\mathcal{A}^\mu - \partial^\mu\mathcal{A}^\nu\right) - ig\left[\mathcal{A}^\mu, \mathcal{A}^\nu\right]. \end{aligned} \tag{1.21}$$

The correct transformtion behaviour of the gauge field $\mathcal{A}^\mu$ can be determined by using (1.16). [4]

[3] Note that γ^μ is a 4D-matrix, thus it does not act on the 3D $U(x)$.

[4] For a more detailed explanation of the made derivations see [10].

1.3 From the Lagrangian to Matrix Element

Before we discuss the different couplings, it is important to have a brief look at how the Lagrangian acts on the matrix element. As the calculation of matrix elements is the primary aspiration of Quantum Field Theory and its use for particle physics, it is useful to picture the connection.
A scattering amplitude from an initial state $|i(t_0)\rangle$ at the time t_0 to a final state $|f(t)\rangle$ at the time t is described by

$$M = \langle f(t)|i(t_0)\rangle = \langle f(t_0')|V^\dagger(t,t_0)|i(t_0)\rangle\,. \tag{1.22}$$

The calculation is made in the interaction picture (Dirac picture). Hence, the Hamiltonian can be split into the Hamiltonian for free particles $H_0(t)$ and an interaction part $H_I(t)$. To make perturbative calculations, we have to assume high energies of the ingoing particles and a small interaction time. For a time-dependent Hamiltonian, the time evolution operator $V(t,t_0)$ can be written as

$$V(t,t_0) = T\left(e^{-i\int_{t_0}^{t} dt' H_I(t')}\right). \tag{1.23}$$

To calculate the scattering amplitude (1.22) we have make a perturbative expansion of (1.23). This is done by the so called Dyson series[5]. We can calculate the Hamiltonian for fields as

$$H = \int d^3x \left(\frac{\partial \mathscr{L}}{\partial(\partial_0\psi)}\partial_0\psi - \mathscr{L}\right). \tag{1.24}$$

To summarize the results: The *matrix element* includes the *time evolution operator* $V(t,t_0)$, which can be expanded according to the Dyson series. Depending on the wanted precision, higher orders of the *Hamiltonian* are included. We can calculate the *Hamiltonian* (1.24) with the *Lagrangian*. Thus the different couplings can already be understood by investigating the Lagrangian.

1.4 Couplings in QCD and QED

To finally investigate how couplings work in QED/QCD, we will inspect the Lagrangians [6]. Starting with the QED Lagrangian

$$\mathscr{L}_{QED} = \hat{\psi}\left(i\gamma^\mu D^\mu - m\right)\psi - \frac{1}{2}F^{\mu\nu}F_{\mu\nu}. \tag{1.25}$$

Inserting the covariant derivative yields

$$\mathscr{L}_{QED} = \underbrace{-\hat{\psi}m\psi + \hat{\psi}i\gamma_\mu\partial^\mu\psi}_{\text{free fermion term}} - \overbrace{\frac{1}{2}F^{\mu\nu}F_{\mu\nu}}^{\text{free photon term}} + \underbrace{ig_e\gamma_\mu\hat{\psi}A^\mu\psi}_{\text{2 fermion-1 photon interaction}}. \tag{1.26}$$

[5] This would end up in a lengthy calculation, which can be looked up in [9].
[6] This was motivated in the previous section.

For the sake of illustration, we can separate the Lagrangian into three parts. The first part describes free fermions, thus called "free fermion term" . Similarly, the second term describes free photons "free photon term". The third term, finally describes the interaction between photons and fermions. [7] This vertex is connected to two fermion fields $\hat{\psi}, \psi$ and one photon field A^μ. Consequently, quantum electrodynamic interactions only occur between fermions and photons. The Feynman graph with the corresponding vertex factor yields:

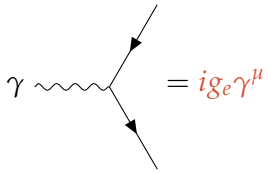

Again, the procedure is similar for the QCD-couplings. Inserting D^μ leads to

$$\mathscr{L}_{QCD} = \underbrace{-\bar{u}mu + \bar{u}i\gamma_\mu\partial^\mu u}_{\text{free quark term}} + \overbrace{ig\bar{u}\gamma_\mu\mathcal{A}^\mu u}^{\text{2 quark, 1 gluon interaction}} \quad -\frac{1}{4}\cdot \underbrace{\text{TR}\left[\mathcal{F}^{\mu\nu}\mathcal{F}_{\mu\nu}\right]}_{\text{gluon interaction term}} .$$

As before, we can identify the "free quark term" and the "quark gluon interaction term". The terms are perfectly analogous, except for the different gauge fields. However, the Lagrangians differ in the last term, which we call "gluon interaction term". This will become particularly important for quantum chromo dynamics, because it represents the self-interaction of gluons.
A closer look at the quark gluon interaction term yields

$$\mathscr{L}_{\text{q,g interaction}} = ig\bar{u}_i\gamma_\mu(T^a_\mu)_{ik}A^\mu_a u_k = ig\gamma_\mu(T^a_\mu)_{ik}\ \bar{u}_i A^\mu_a u_k. \tag{1.27}$$

Similar to the previous calculation, we can illustrate the quark gluon interaction in a Feynman diagram:

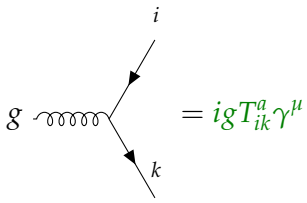

Now we can investigate the gluon interaction term. *The factor* $-1/4$ *and the trace are ignored for now.* Including the definition for the field strength tensor (1.20) yields

$$\mathscr{L}_{\text{Gluon interaction}} = \left[\left(\partial^\nu\mathcal{A}^\mu - \partial^\mu\mathcal{A}^\nu\right) - ig\left[\mathcal{A}^\mu, \mathcal{A}^\nu\right]\right]\cdot\left[\left(\partial_\nu\mathcal{A}_\mu - \partial_\mu\mathcal{A}_\nu\right) - ig\left[\mathcal{A}_\mu, \mathcal{A}_\nu\right]\right] \tag{1.28}$$

[7] Only fermions with an electric charge are affected.

Because of the addition $ig\left[\mathcal{A}^\mu, \mathcal{A}^\nu\right]$, the Lagrangian differs from the QED results. Multiplying this out results in the three different terms

$$\begin{aligned}\mathscr{L}_{\text{gluon interaction}} = &\underbrace{-g^2[\mathcal{A}^\mu, \mathcal{A}^\nu][\mathcal{A}_\mu, \mathcal{A}_\nu]}_{\text{4 gluon interaction}} \\ &\underbrace{- ig\left[\mathcal{A}^\mu, \mathcal{A}^\nu\right]\left(\partial_\nu \mathcal{A}_\mu - \partial_\mu \mathcal{A}_\nu\right) - ig\left(\partial^\nu \mathcal{A}^\mu - \partial^\mu \mathcal{A}^\nu\right)\left[\mathcal{A}_\mu, \mathcal{A}_\nu\right]}_{\text{3 gluon interaction term}} \\ &\underbrace{+ \left(\partial^\mu \mathcal{A}^\nu \partial_\mu \mathcal{A}_\nu - \partial^\mu \mathcal{A}^\nu \partial_\nu \mathcal{A}_\mu\right)}_{\text{free gluon term}}.\end{aligned} \tag{1.29}$$

The "free gluon term" is similar to the "free photon term" in QED. In contrast, we can identify self-coupling terms of the gluons. The calculations are a bit lengthy and can be looked up in Appendix B.[8]
The 3-gluon coupling term reads:

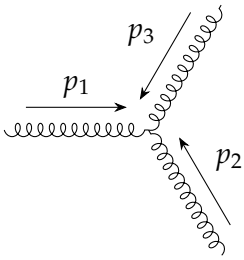

$$= -gf^{abc}\left(g_{\mu\nu}\left(p_1 - p_2\right)_\lambda + g_{\nu\lambda}\left(p_2 - p_3\right)_\mu + g_{\lambda\mu}\left(p_3 - p_1\right)_\nu\right)$$

The 4-gluon coupling term reads:

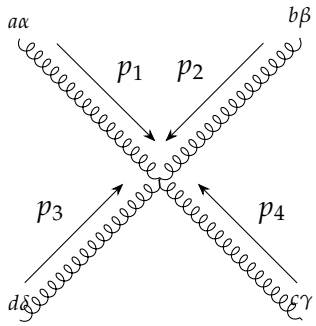

$$= -ig^2\left[\begin{array}{l} f^{\text{abe}} f^{\text{cde}}\left(g^{\alpha\gamma}g^{\beta\delta} - g^{\alpha\delta}g^{\beta\gamma}\right) \\ + f^{ace} f^{bde}\left(g^{\alpha\beta}g^{\gamma\delta} - g^{\alpha\delta}g^{\gamma\beta}\right) \\ + f^{ade} f^{bce}\left(g^{\alpha\beta}g^{\delta\gamma} - g^{\alpha\gamma}g^{\delta\beta}\right) \end{array}\right]$$

[8] For the calculations, the trace has to be considered again.

2 Strong coupling constant

The direct photon production includes strong interactions, which significantly depend on the energy scale of the process. At short distances, the strong coupling constant can be calculated in the first approximation as

$$\alpha_s\left(Q^2\right) = \frac{4\pi}{\beta_0 \ln\left(Q^2/\Lambda^2\right)}. \tag{2.1}$$

[1] Λ^2 and β_0 are given by

$$\Lambda^2 = \mu^2 e^{-\frac{4\pi}{\beta_0 \alpha_s\left(\mu^2\right)}} \qquad \beta_0 = 11 - \frac{2}{3} n_f. \tag{2.2}$$

n_f describes the number of quark flavours wich participate in the process. Considering (2.2), the strong coupling depends only on the energy scale Q^2 and μ. We can choose μ according to [3]

$$\mu = M_z = 91.18 \text{ GeV}; \quad \alpha_s(\mu^2) = \alpha_s(M_z^2) = 0.1181. \tag{2.3}$$

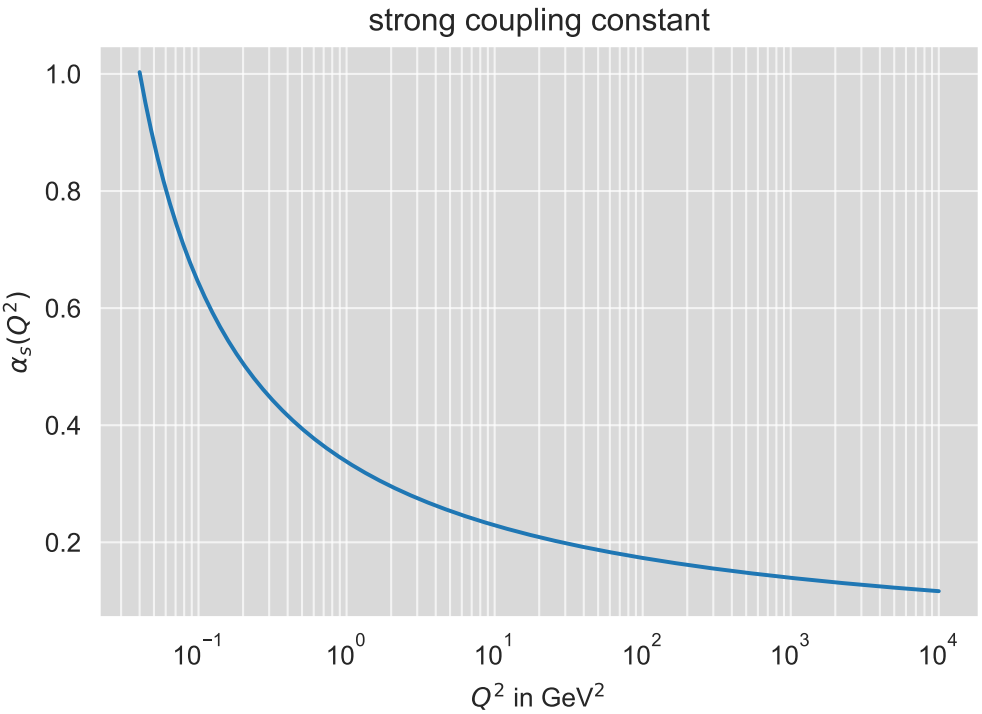

Figure 1: Strong coupling constant $\alpha_s(Q^2)$ in dependence of Q^2.

3 PDFs

The cross section, described in section 4, is defined for particles like gluons and quarks. Unfortunately, because of the confinement principle, quarks can not exist as free states. If we want to observe these particles, it is necessary to observe them in major particles with an inner structure like protons. A proton consists of three valence quarks which dominate especially at lower energy scales and so-called sea quarks, which occur at higher energy scales. Moreover, quarks interact via strong interaction by exchanging gluons.[9] Just like quarks, gluons are partons as well, and also participate in interactions.

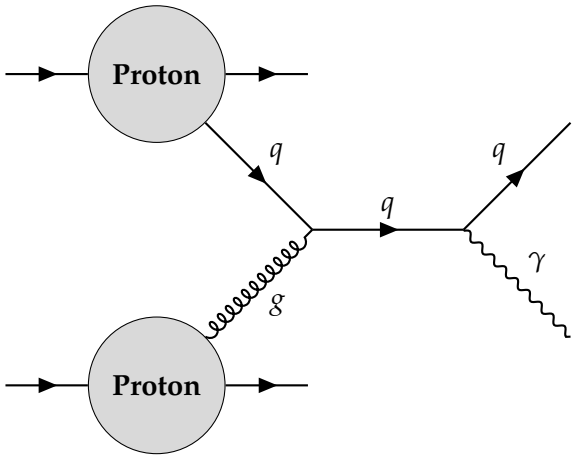

Figure 2: The Feynman diagram of hard compton scattering in a proton-proton-collision.

The made calculations only apply to single quarks and gluons (so-called partons), which can not be observed directly in the experiment. Therefore, the parton model is used, which describes the quarks and gluons as constituents of the proton. In the event of a collision, a parton with a certain momentum fraction $[x, x + dx]$ can interact with a certain probability $f(x)dx$. The function $f(x)$ describes the probability density for the parton and is therefore called parton distribution function or in short PDF. Translating the matrix elements for free quarks and gluons to the proton frame yields

$$\sigma_{proton} = \sum_{a,b} \int \underbrace{dx_1 dx_2 f_a(x_1, Q) f_b(x_2, Q)}_{\text{probability to observe partons a and b in } dx_1 dx_2 \text{ at an energy scale Q}} \hat{\sigma}_{ab}(x_1, x_2) \tag{3.1}$$

Of course, the probability density varies on different energy scales Q, since sea quarks and gluons can only be observed at small distances.

[9] This was discussed in section 1.

The proton-PDF-sets are shown in Figure 3, on different energy scales. When we treat protons we assume 5 different quarks.

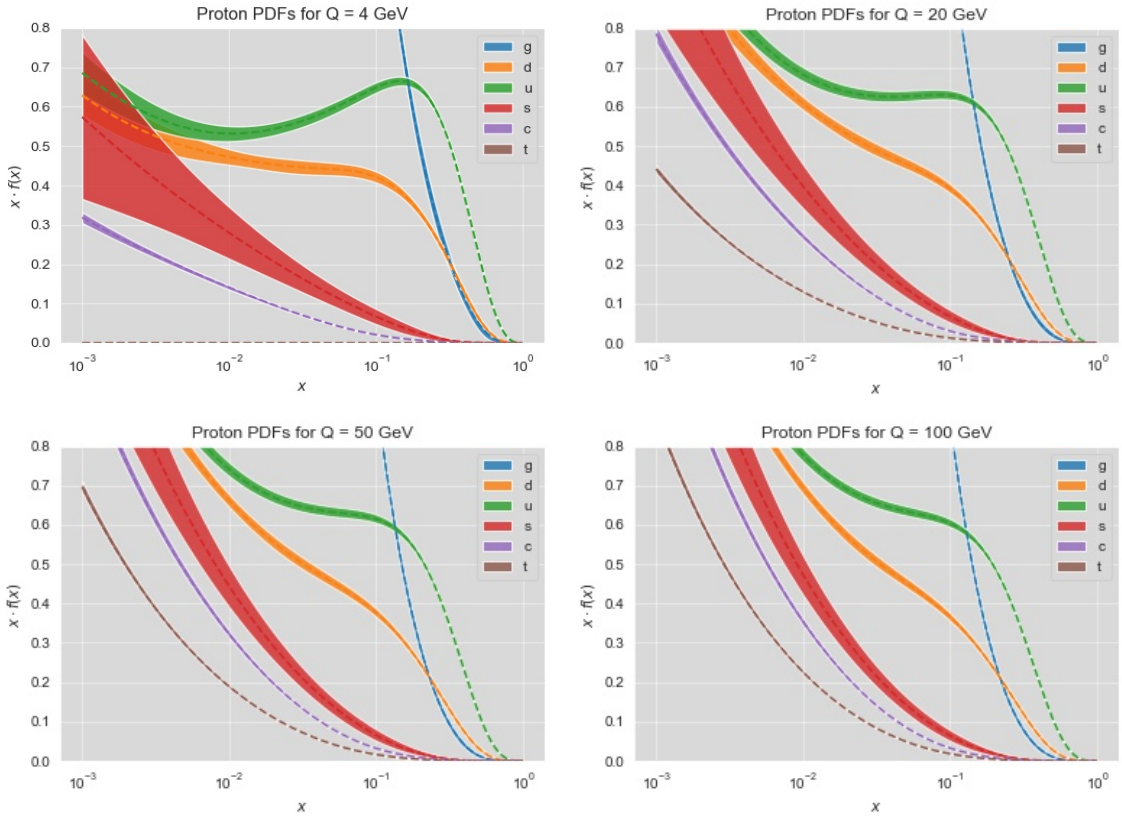

Figure 3: Proton-PDF $xf(x)$ for energy scales $Q = 4, 20, 50, 100$ GeV in dependence of the momentum fracion x. The PDFs are taken from [6].

For higher energy scales Q, the PDF-values increase due to the higher probability of receiving sea quarks. The probability for high x is dominated by the valence quarks of the proton (up and down). Hence, higher energy scales have only a small influence on the PDF values at high x. [10]

[10] In contrast to low x, we can observe a decrease of $f(x)$ here.

4 Cross-Section

To prove theoretical calculations, we have to compare the results with experiments. Because, we can not measure Lagrangians or matrix elements, a new quantity is needed, which characterises the interactions. This is provided by the so-called cross section. If we perform a classical scattering experiment [11] the cross section is simply related to the radius of the particles. In quantum mechanics or quantum field theory, where we speak of particles in terms of waves and fields, it is a more abstract term. However, it can still be interpreted as an effective area which characterises the process, independent from our frame of reference or the number of measured events.
We can write the differential cross section in terms of the Lorentz invariant phase space element dP_n, the initial flux F and the matrix elements M

$$d\sigma = \frac{|M|^2}{F} \cdot dP_n. \tag{4.1}$$

The initial flux F is given by

$$F = |\mathbf{v}_A| \, 2E \cdot 2E'. \tag{4.2}$$

The relative velocity $|\mathbf{v}_A|$ can be written as $|\mathbf{v}_A| = |p/E - p'/E'|$, thus for high energies we can assume $p \approx E \Rightarrow |\mathbf{v}_A| \approx 2$.[12] This is no measurable quantity, since nothing can travel faster than light. The next assumption for the following calculations is $E = E'$, which yields

$$F = 4E^2 = 2s_{cm}. \tag{4.3}$$

The Lorentz invariant phase space element (LIPS) dP_n is given by [5]

$$dPS_n \equiv (2\pi)^4 \delta^{(4)} \left(P - \sum_{i=1}^{n} p_i \right) \Pi_{i=1}^{n} \frac{1}{(2\pi)^3} \frac{d^3\vec{p}_i}{2E_i}. \tag{4.4}$$

The delta function expresses the four momentum conservation of the process. To see that the LIPS is indeed Lorentz invariant is straight forward. The delta function simply states the energy-momentum conservation and is clearly invariant under Lorentz transformation. The calculation for d^3p/E is done in subsection A.5 and is important to note for section 6.
Finally, the differential cross section for two outgoing particles under the imposed conditions yields

$$d\sigma = \frac{|M|^2}{2s} \cdot \delta^{(4)} \left(P - \sum_{i=1}^{n} p_i \right) \frac{1}{(2\pi)^2} \frac{d^3p_1}{2E_1} \frac{d^3p_2}{2E_2}. \tag{4.5}$$

[11] For example Helium atoms on a gold foil, with a cross section of $\sigma = \pi r^2$.
[12] This is written in natural units and simply states that v $\rightarrow$c.

5 Matrix Elements

Direct photons can be produced at leading order in the 3 following processes, which all contain a photon and a gluon. Thus, for direct photon production, both strong and electromagnetic interactions have to be considered.

5.1 Quark-Gluon ⇒ Quark-Photon

This process is the major process in leading order direct photon production, as we will see in section section 8. It is called hard Compton scattering, since we simply have to exchange a virtual photon with a gluon to obtain the Feynman diagram from the Compton scattering.

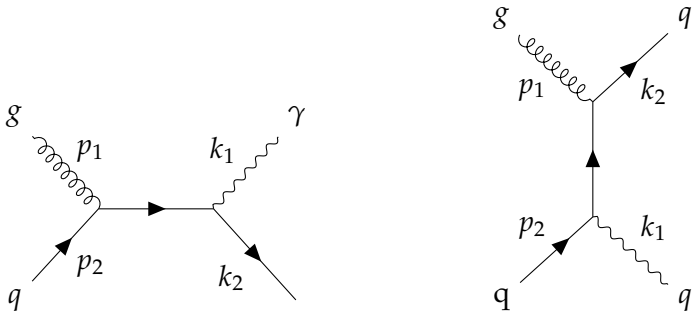

Figure 4: Tree-level Feynman diagrams for the quark-gluon to quark-γ process.

The purpose of the following calculation is to determine the transition amplitude probability for different processes, which is described by the matrix element (more precisely, by $\overline{|M|^2}$). The matrix element has to be averaged (which is symbolized by the overline), because the ingoing particles are totally unpolarized. That includes averaging the spins of ingoing fermions, polarizations of ingoing bosons and color of the ingoing quarks and gluons. The averaged $\overline{|M|^2}$ is given by

$$\overline{|M|^2} = \overline{|M_s|^2} + \overline{|M_u|^2} + \overline{2\,\mathrm{Re}\left\{M_s M_s^\dagger\right\}}. \tag{5.1}$$

To calculate (5.1), the matrix elements for the u- and s-channel have to be determined. The following expressions are calculated according to the Feynman rules, outlined in subsection A.4

$$\begin{aligned} M_s &= \bar{u}\left(k_2\right)\left(-ieQ\gamma_\nu\right)\varepsilon_s^\mu(k_1)\frac{i(\not{p}_s + m)}{s - m^2}\varepsilon_r^{\mu^*}\left(p_1\right)\left(ig\gamma_\mu T^a\right)u\left(p_1\right) \\ &= T^a\varepsilon_s^\mu(k_1)\varepsilon_r^{\mu^*}\left(p_1\right)\left(ieQg\right)\bar{u}\left(k_2\right)\gamma_\nu\frac{(\not{p}_s + m)}{s - m^2}\gamma_\mu u\left(p_2\right). \end{aligned} \tag{5.2}$$

The adjoint matrix elements can the be obtained by straightforward calculation from (5.2)

$$M_s^\dagger = T^b\varepsilon_r^\sigma\left(p_1\right)\varepsilon_s^{\rho^*}\left(k_1\right)\left(-ieQg\right)\bar{u}\left(p_2\right)T^b\gamma_\sigma\frac{(\not{p}_s + m)}{s - m^2}\gamma_\rho u\left(k_2\right). \tag{5.3}$$

For the u-channel, the matrix elements can be obtained anlogically

$$M_u = T^a \varepsilon_s^{\mu}(k_1)\varepsilon_r^{\nu^*}(p_1)\,(ieQg)\,\bar{u}(k_2)\gamma_\nu \frac{(\not{p}_u + m)}{u - m^2}\gamma_\mu u\,(p_2) \tag{5.4}$$

$$M_u^\dagger = T^b \varepsilon_s^{\rho}(p_1)\varepsilon_r^{\sigma^*}(k_1)\,(-ieQg)\,\bar{u}\,(p_2)\,T^b\gamma_\sigma \frac{(\not{p}_u + m)}{u - m^2}\gamma_\rho u\,(k_2)\,. \tag{5.5}$$

The matrix element (5.1) can be calculated in three steps by calculating the 3 terms separately. $|M_S|^2$ is obtained by multiplying (5.2) and (5.3)

$$\begin{aligned}|M_s|^2 =& M_s \cdot M_s^\dagger = T^a T^b \varepsilon_s^{\nu}(k_1)\varepsilon_r^{\mu^*}(p_1)\varepsilon_r^{\sigma}(p_1)\varepsilon_s^{\rho^*}(k_1)\,(eQg)^2 \\ & \bar{u}\,(k_2)\,\gamma_\nu \frac{(\not{p}_s + m)}{s - m^2}\gamma_\mu u\,(p_2)\,\bar{u}\,(p_2)\,\gamma_\sigma \frac{(\not{p}_s + m)}{s - m^2}\gamma_\rho u\,(k_2)\,.\end{aligned} \tag{5.6}$$

To get the average, all possible variations have to be summed up and divided by the total number of possible variations. As mentioned before, that includes the spin of quarks, polarization of bosons r, s and the color a, b of strong couplings

$$\begin{aligned}\overline{|M_s|^2} =& \frac{(eQg)^2}{(s-m^2)^2}\frac{1}{2}\sum_{r,s}\varepsilon_s^{\nu}(k_1)\varepsilon_s^{\rho^*}(k_1)\varepsilon_r^{\mu^*}(p_1)\varepsilon_r^{\sigma}(p_1) \\ & \frac{1}{2}\sum_{\text{spins}}\bar{u}\,(k_2)\,\gamma_\nu\,(\not{p}_s + m)\,\gamma_\mu u\,(p_2)\,\bar{u}\,(p_2)\,\gamma_\sigma\,(\not{p}_s + m)\,\gamma_\rho u\,(k_2) \\ & \frac{1}{N(N-1)}\sum_{a,b}T^a T^b.\end{aligned} \tag{5.7}$$

The color average affects only the SU(N) generators T_a and can therefore be calculated separately according to subsection A.2. Carrying out the summations by using the completeness relations (A.1) and polarization sum (A.3) yields

$$\overline{|M_s|^2} = \frac{(eQg)^2}{(s-m^2)^2}\cdot\frac{1}{4}\cdot\frac{1}{2N}\cdot g^{\gamma\rho}g^{\sigma\mu}\cdot \mathrm{TR}\left[(\not{k}_2 + m)\gamma_v(\not{p}_s + m)\gamma_\mu(\not{p}_2 + m)\gamma_\sigma(\not{p} + m)\gamma_\rho\right]. \tag{5.8}$$

Next, we have to calculate the trace by using trace theorems subsection A.3. Multiplying out the bracket results in $2^8 = 16$ different traces, which are proportional to m^0, m^1, m^2, m^3 and m^4. Traces with odd numbers of gamma matrices vanish, i.e. by considering only even numbers of gamma matrices which leads to even powers of m, the number of traces reduces to 8.

We can classify the calculations by traces $\propto m^0, m^2$ and m^4:

$$\begin{aligned}
&\text{Traces} \propto m^0\text{:}\\
\text{TR}\left[\not{k}_2\gamma^\rho \not{p}\gamma_\sigma \not{p}\gamma_\rho\right] &= k_{2,\alpha}p_\beta p_{2,\lambda}p_\delta \,\text{TR}[\underbrace{\gamma^\sigma\gamma^\lambda\gamma_\sigma}_{=-2\gamma^\lambda}\gamma^\delta\underbrace{\gamma_\rho\gamma^\alpha\gamma^\rho}_{=-2\gamma^\alpha}\gamma^\beta]\\
&= 4k_{2,\alpha}p_\beta p_{2,\lambda}p_\delta \,\text{TR}\left[\gamma^\alpha\gamma^\beta\gamma^\lambda\gamma^\delta\right] =\\
&= 16\,(k_2p_s)\,(p_2p_s) - (k_2p_2)\,(p_sp_s)
\end{aligned}$$

$$\text{Traces} \propto m^2\text{:}$$

$$\begin{aligned}
\text{TR}\left[\not{k}_2\gamma^\rho \not{p}\gamma^\sigma\gamma_\sigma\gamma_\rho\right] &= -8k_2^\alpha p^\beta \,\text{TR}\left[\gamma_\alpha\gamma_\beta\right] = -32k_2\cdot p\\
\text{TR}\left[\not{k}_2\gamma^\rho\gamma^\sigma \not{p}_2\gamma_\sigma\gamma_\rho\right] &= 4k_2^\alpha p_2^\beta \,\text{TR}\left[\gamma_\alpha\gamma_\beta\right] = 16k_2\cdot p_2\\
\text{TR}\left[\not{k}_2\gamma^\rho\gamma^\sigma\gamma_\sigma \not{p}\gamma_\rho\right] &= -8k_2^\alpha p_2^\beta \,\text{TR}\left[\gamma_\alpha\gamma_\beta\right] = -32k_2\cdot p\\
\text{TR}\left[\gamma^\rho \not{p}\gamma^\sigma \not{p}_2\gamma_\sigma\gamma_\rho\right] &= -8p^\alpha p_2^\beta \,\text{TR}\left[\gamma_\alpha\gamma_\beta\right] = -32k_2\cdot p_2\\
\text{TR}\left[\gamma^\rho \not{p}\gamma^\sigma\gamma_\sigma \not{p}\gamma_\rho\right] &= 64p\cdot p\\
\text{TR}\left[\gamma^\rho\gamma^\sigma \not{p}_2\gamma_\sigma \not{p}\gamma_\rho\right] &= -8k_2^\alpha p_2^\beta \,\text{TR}\left[\gamma_\alpha\gamma_\beta\right] = -32p_2\cdot p
\end{aligned}$$

$$\text{Traces} \propto m^4\text{:}$$

$$\text{TR}\left[\gamma^\rho\gamma^\sigma\gamma_\sigma\gamma_\rho\right] = 64$$

Calculating $\overline{|M_u|^2}$ yields the same expression as (5.8), since the only difference between the matrix elements M_u and M_s consists in an exchange of indices of the polarization vectors. Thus it can not affect the calculation of $\overline{|M_u|^2}$, since the indices are changed respectively in $M_s^\dagger$

$$\begin{aligned}
\overline{|M_u|^2} =& \frac{(eQg)^2}{(s-m^2)^2}\frac{1}{2}\sum_{r,s}\varepsilon_s^\mu(k_2)\varepsilon_s^{\sigma^*}(k_2)\varepsilon_r^{\nu^*}(p_2)\varepsilon_r^\rho(p_2)\\
&\frac{1}{2}\sum_{\text{spins}}\bar{u}\,(k_2)\,\gamma_\nu\left(\not{p}_u+m\right)\gamma_\nu u\,(p_2)\,\bar{u}\,(p_2)\,\gamma_\rho\left(\not{p}_u+m\right)\gamma_\sigma u\,(k_2)\\
&\frac{1}{N(N-1)}\sum_{a,b}T^aT^b\\
=& \frac{(eQg)^2}{(u-m^2)^2}\cdot\frac{1}{4}\cdot\frac{1}{2N}\cdot\text{TR}\left[(\not{k}_2+m)\gamma_v(\not{p}_u+m)\gamma_\mu(\not{p}_2+m)\gamma_\sigma(\not{p}_u+m)\gamma_\rho\right]. \quad (5.9)
\end{aligned}$$

Because of that, the traces can be calculated in the same way, substituting $s \to u$. Finally,

we obtain the mixed-term by multiplying and averaging (5.2) with (5.5)

$$\begin{aligned}\overline{2\,\mathrm{Re}\left\{M_s M_s^{\dagger}\right\}} = &\frac{(eQg)^2}{(s-m^2)\,(u-m^2)}\frac{1}{2}\sum_{r,s}\varepsilon_s^{\nu}(k_1)\varepsilon_s^{\sigma^*}(k_1)\varepsilon_r^{\mu^*}(p_1)\varepsilon_r^{\rho}(p_1) \\ &\frac{1}{2}\sum_{\text{spins}}\bar{u}\,(k_2)\,\gamma_\nu\left(\not{p}_s+m\right)\gamma_\mu u\,(p_2)\,\bar{u}\,(p_2)\,\gamma_\sigma\left(\not{p}_u+m\right)\gamma_\rho u\,(k_2) \\ &\frac{1}{N(N-1)}\sum_{a,b}T^aT^b.\end{aligned} \tag{5.10}$$

The color calculation is identical to the previous one. Again, we have to carry out the summations by applying the completeness relations and polarization sums

$$\begin{aligned}\overline{2\,\mathrm{Re}\left\{M_s M_s^{\dagger}\right\}} = &\frac{(eQg)^2}{(s-m^2)\,(u-m^2)}\frac{1}{2}\cdot\frac{1}{2N}\cdot g^{\sigma\nu}g^{\rho\mu} \\ &\mathrm{TR}\left[(\not{k}_2+m)\gamma_v(\not{p}_s+m)\gamma_\mu(\not{p}_2+m)\gamma_\sigma(\not{p}_u+m)\gamma_\rho\right].\end{aligned} \tag{5.11}$$

Terms proportional to m^0, m^2 and m^4 occur:

traces $\propto m^0$

$$\begin{aligned}\mathrm{TR}\left[\not{k}_2\gamma_\nu\not{p}_s\gamma_\mu\not{p}_2\gamma^\nu\not{p}_u\gamma^\mu\right] &= k_2^\alpha p_s^\beta p_2^\sigma p_u^\rho\,\mathrm{TR}\left[\gamma^\alpha\gamma_\nu\gamma^\beta\gamma_\mu\gamma^\sigma\gamma^\nu\gamma^\rho\gamma^\mu\right] \\ &= k_2^\alpha p_s^\beta p_2^\sigma p_u^\rho(-2)\,\mathrm{TR}\left[\gamma^\alpha\gamma_\nu\gamma^\beta\gamma^\sigma\gamma^\nu\gamma^\rho\right] = -32(k_2\cdot p_2)(p_s\cdot p_u)\end{aligned}$$

traces $\propto m^2$

$$\begin{aligned}\mathrm{TR}\left[\not{k}_2\gamma_\nu\not{p}_s\gamma_\mu\gamma^\nu\gamma^\mu\right] &= 4\,\mathrm{TR}\left[\not{k}_2\not{p}_s\right] = 16k_2\cdot p_s \\ \mathrm{TR}\left[\not{k}_2\gamma_\nu\gamma_\mu\not{p}_2\gamma^\nu\gamma^\mu\right] &= k_2^\alpha p_{2\beta}\,\mathrm{TR}\left[\gamma_\alpha\gamma_\nu\gamma_\mu\gamma^\beta\gamma^\nu\gamma^\mu\right] \\ &= k_2^\alpha p_{2\beta}4\,\mathrm{TR}\left[g_{\alpha\mu}\gamma^\beta\gamma^\mu\right] = 16k_2\cdot p_2 \\ \mathrm{TR}\left[\not{k}_2\gamma_\nu\gamma_\mu\gamma^\nu\not{p}_u\gamma^\mu\right] &= k_{2\alpha}p_u^\beta(-2)\,\mathrm{TR}\left[\gamma^\alpha\gamma_\mu\gamma_\beta\gamma^\mu\right] = 16k_2\cdot p_u \\ \mathrm{TR}\left[\gamma_\nu\not{p}_s\gamma_\mu\not{p}_2\gamma^\nu\gamma^\mu\right] &= -2pp_2\,\mathrm{TR}\left[\gamma^\mu\gamma^\rho\gamma_\mu\gamma_\rho\right] = 16p_s\cdot p_2 \\ \mathrm{TR}\left[\gamma_\nu\not{p}_s\gamma_\mu\not{p}_2\gamma^\nu\gamma^\mu\right] &= 16p_s\cdot p_u \\ \mathrm{TR}\left[\gamma_\nu\gamma_\mu\not{p}_2\gamma^\nu\not{p}_u\gamma^\mu\right] &= p_2\cdot p_u\end{aligned}$$

traces $\propto m^4$

$$\mathrm{TR}\left[\gamma_\nu\gamma_\mu\gamma^\nu\gamma^\mu\right] = -2\,\mathrm{TR}\left[\gamma_\mu\gamma^\mu\right] = -32$$

Adding up the three parts leads to the matrix element

$$\begin{aligned}
\overline{|M|^2} &= \overline{|M_s|^2} + \overline{|M_u|^2} + \overline{2\,\mathrm{Re}\,\{M_s M_s^\dagger\}} = \\
&\frac{(eQg)^2}{(s-m^2)^2}\cdot\frac{4}{2N}[4m^4 + m^2(k_2p_2 + 4p_sp_s - 4k_2p - 4p_2p_s) + \\
&2(k_2p_s)(p_2p_s) - (k_2p_2)(p_sp_s)] + \frac{(eQg)^2}{(u-m^2)^2}\cdot\frac{4}{2N}[4m^4 + m^2(k_2p_2 + 4p_up_u - 4k_2p_u - 4p_2p_u) + \\
&2(k_2p_u)(p_2p_u) - (k_2p_2)(p_up_u)] + \frac{(eQg)^2}{(u-m^2)(s-m^2)} \\
&\frac{4}{2N}[-4m^4 + 2m^2(k_2p_s + k_2p_1 + k_2p_u + p_sp_2 + p_up_s + p_2p_u) \\
&- 32(k_2p_2)(p_up_s)].
\end{aligned} \tag{5.12}$$

The quarks (up, down and strange) which occur in this process hold masses at a scale of $(10^0 - 10^2)$ MeV, which is negligible compared to the quark momentum at a scale of GeV. Besides this, only m^2 and m^4 appear in the calculation, which increases the factor between quark masses and momentum up to 6 orders of magnitude.
With the simplification $m_{quark} \approx 0$ the matrix-element is reduced to

$$\begin{aligned}
\overline{|M|^2} = (eQg)^2\cdot\frac{1}{4}\cdot\frac{1}{2N}\cdot 16\Bigg[&\frac{2\,(k_2\cdot p_s)\,(p_2\cdot p_s) - (k_2\cdot p_s)\,p_s^2}{s^2} + \\
&\frac{2\,(k_2\cdot p_u)\,(p_2\cdot p_u) - (k_2\cdot p_2)\,p_u^2}{u^2} - 4\cdot\frac{(k_2\cdot p_2)\,(p_s\cdot p_u)}{us}\Bigg].
\end{aligned} \tag{5.13}$$

Additionally, we can simplify the Mandelstam variables

$$s = (p_1 + p_2)^2 \approx 2p_1p_2 \tag{5.14}$$

$$u = (p_2 - k_1)^2 = (p_1 - k_2)^2 \approx -2p_2k_1 \approx -2p_1k_2 \tag{5.15}$$

$$t = (p_2 - k_2)^2 = (p_1 - k_1)^2 \approx -2p_2k_2 \approx -2p_1k_1. \tag{5.16}$$

Identifying the Mandelstam variables with the matrix element (5.13) yields

$$\begin{aligned}
\overline{|M|^2} &= (eQg)^2\cdot\frac{1}{4}\cdot\frac{1}{2N}\cdot 16\left[\frac{1}{2}\left(\frac{(-u-t)s + ts}{s^2} + \frac{(-t+u)u + tu}{u^2}\right) + 2t(u+s+t)\right] \\
&= -\frac{(eQg)^2}{N}\left[\frac{u^2+s^2}{us} - 2t(u+s+t)\right].
\end{aligned} \tag{5.17}$$

5.2 Anti Quark-Gluon ⇒ Anti Quark-Gamma

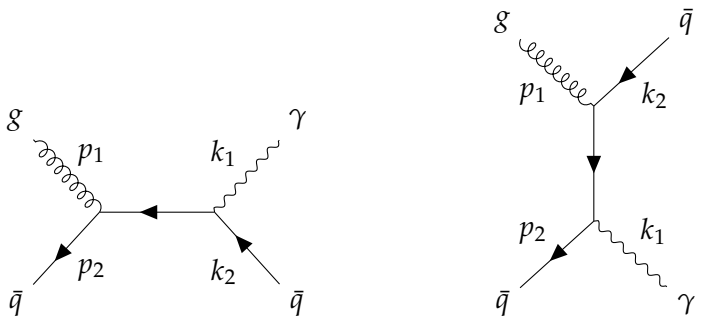

Figure 5: Tree-level Feynman diagrams for the antiquark-gluon to antiquark-γ process. s-channel (left) and u-channel (right)

The calculation of the matrix element from the second process proceeds similar to the previous one. Since the processes only differ in the appearance of antiquarks instead of quarks, the matrix elements $M_s, M_s^\dagger, M_u, M_u^\dagger$ can simply be obtained by using v-spinors. For example (5.2) can be expressed as

$$\overline{|M_s|^2} = T^a \varepsilon_s^\mu(k_1) \varepsilon_r^{\mu^*}(p_1) \, (ieQg) \, \bar{v}(k_2) \, \gamma_\nu \frac{(\not{p}_s + m)}{s - m^2} \gamma_\mu v(p_2) \tag{5.18}$$

Due to the spin sum and the completeness relation (A.1), only the sign of m in the traces changes from $+ \rightarrow -$. As only even powers of mass terms exist, the calculation is identical even without the simplification $m_{quark} = 0$

$$\not{p} + m \rightarrow \not{p} - m.$$

So we can assume

$$\begin{aligned} \overline{|M|^2}_{qg \rightarrow q\gamma} &= \overline{|M|^2}_{\bar{q}g \rightarrow \bar{q}\gamma} \\ &= -\frac{(eQg)^2}{N} \left[\frac{u^2 + s^2}{u \, s} - 2t(u + s + t) \right]. \end{aligned} \tag{5.19}$$

5.3 Quark-Anti Quark ⇒ Gluon-Gamma

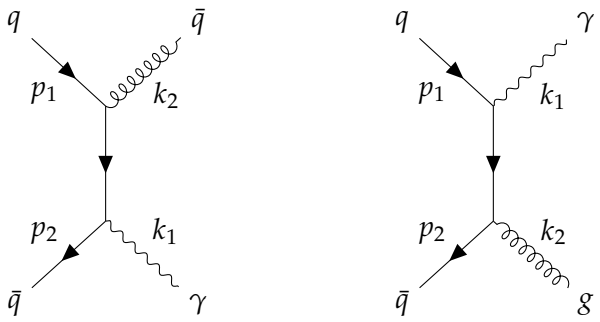

Figure 6: Tree-level Feynman diagrams for the quark-antiquark annihilation. t-channel (left) and u-channel (right)

Third, the matrix elements for quark-antiquark annihilation have to be calculated. Since the masses are negligible, there is no need to do this calculation without this simplification.
The matrix elements of the t- and u-channel are given by

$$M_t = T^a \varepsilon_s^\nu(k_2) \varepsilon_r^{\mu^*}(k_1) \, (ieQg) \, \bar{v}(p_2) \gamma_\nu \frac{(\not{p}_1 - \not{k}_1)}{t} \gamma_\mu u(p_1) \tag{5.20}$$

$$M_t^\dagger = T^b \varepsilon_s^\sigma(k_1) \varepsilon_r^{\rho^*}(k_2) \, (-ieQg) \, \bar{v}(p_1) \gamma_\sigma \frac{(\not{p}_1 - \not{k}_1)}{t} \gamma_\rho u(p_2) \tag{5.21}$$

$$M_u = T^a \varepsilon_s^\nu(k_1) \varepsilon_r^{\mu^*}(k_2) \, (ieQg) \, \bar{v}(p_2) \gamma_\nu \frac{(\not{p}_1 - \not{k}_2)}{u} \gamma_\mu u(p_1) \tag{5.22}$$

$$M_u^\dagger = T^b \varepsilon_s^\sigma(k_2) \varepsilon_r^{\rho^*}(k_1) \, (-ieQg) \, \bar{v}(p_1) \gamma_\sigma \frac{(\not{p}_1 - \not{k}_2)}{u} \gamma_\rho u(p_2) \, . \tag{5.23}$$

Analogously to (5.1) we can calculate the the matrix element in three steps and the color dependent part can be calculated separately. Using the relations from subsection A.2 the color term yields

$$\frac{1}{N^2} \sum_{a,b} T_a T_b = \frac{N^2 - 1}{2N^2}. \tag{5.24}$$

Now we can calculate $\overline{|M_t|^2}$

$$\begin{aligned} \overline{|M_t|^2} =& \frac{N^2-1}{2N^2} \cdot \frac{1}{4} \cdot \frac{(eQg)^2}{t^2} \sum_{r,s} \varepsilon_r^\nu(k_2) \, \varepsilon_s^{\mu^*}(k_1) \, \varepsilon_r^{\rho^*}(k_2) \, \varepsilon_s^\sigma(k_1) \\ & \sum_{spin} \bar{v}(p_2) \gamma^r p_t \gamma^\mu u(p_1) \, \bar{u}(p_1) \gamma^\sigma p_t \gamma^\rho v(p_2) \end{aligned} \tag{5.25}$$

$$= \frac{N^2-1}{2N^2} \cdot \frac{1}{4} \cdot \frac{(eQg)^2}{t^2} g^{\nu\sigma} g^{\mu\rho} \, \mathrm{TR}\left[\not{p}_2 \gamma_\nu \not{p}_u \gamma_\mu \not{p}_1 \gamma_\sigma \not{p}_u \gamma_\rho\right]. \tag{5.26}$$

As before, the trace is calculated according to the trace theorems subsection A.3

$$\begin{aligned}\mathrm{TR}\left[\not{p}_2\gamma^\rho\not{p}_t\gamma^\sigma\not{p}_1\gamma_\sigma\not{p}t\gamma_\rho\right] &= p_2^\alpha p_t^\beta p_1^\nu p_t^\mu \,\mathrm{TR}\left[\gamma_\alpha\gamma^\rho\gamma_\beta\gamma^\sigma\gamma_\nu\gamma_\sigma\gamma_\mu\gamma_\rho\right]\\ &= p_2^\alpha p_t^\beta p_1^\nu p_t^\mu 4\,\mathrm{TR}\left[\gamma_\alpha\gamma_\beta\gamma_\nu\gamma_\mu\right]\\ &= 16\left((p_2p_t)(p_1p_t)-(p_2p_1)p_t^2+(p_2p_t)(p_1p_t)\right). \end{aligned} \tag{5.27}$$

Inserting the mandelstamvariables into (5.27) yields

$$\mathrm{TR}\left[\not{p}_2\gamma^\rho\not{p}_t\gamma^\sigma\not{p}_1\gamma_\sigma\not{p}t\gamma_\rho\right] = 16\cdot\frac{((s+u)t-2st+(s+u)t)}{4} = 8tu. \tag{5.28}$$

The calculation of $\overline{|M_u|^2}$ is analogous to the previous one, because of the double exchange of indices $\mu \rightleftarrows \nu$ and $\rho \rightleftarrows \sigma$

$$\begin{aligned}\overline{|M_u|^2} =& \frac{N^2-1}{2N^2}\cdot\frac{1}{4}\cdot\frac{(eQg)^2}{u^2}\sum_{r,s}\varepsilon_r^{\mu^*}(k_2)\,\varepsilon_s^\nu(k_1)\,\varepsilon_r^\sigma(k_2)\,\varepsilon_s^{\rho^*}(k_1) \qquad (5.29)\\ &\sum_{spin}\bar v(p_2)\,\gamma^r p_t\gamma^\mu u(p_1)\,\bar u(p_1)\,\gamma^\sigma p_t\gamma^\rho v(p_2)\\ =& \frac{N^2-1}{2N^2}\cdot\frac{1}{4}\cdot\frac{(eQg)^2}{u^2}g^{\nu\sigma}g^{\mu\rho}\,\mathrm{TR}\left[\not{p}_2\gamma_\nu\not{p}_u\gamma_\mu\not{p}_1\gamma_\sigma\not{p}_u\gamma_\rho\right]. \qquad (5.30)\end{aligned}$$

So the trace is similar to the previous one. An exchange of $t \rightleftarrows u$ in the propagator will be sufficient

$$\begin{aligned}\mathrm{TR}\left[\not{p}_2\gamma^\rho\not{p}_t\gamma^\sigma\not{p}_1\gamma_\sigma\not{p}t\gamma_\rho\right] &= 16\left((p_2p_u)(p_1p_u)-(p_2p_1)p_t^2+(p_2p_u)(p_1p_u)\right)\\ &= 16\frac{((s+t)u-2su+(s+t)u)}{4} = 8tu.\end{aligned}$$

Finally, the mixed term yields

$$\begin{aligned}\overline{2\cdot\mathrm{Re}\left\{M_tM_u^\dagger\right\}} =& 2\cdot\frac{N^2-1}{2N^2}\cdot\frac{1}{4}\cdot\frac{(eQg)^2}{ut}\sum_{r,s}\varepsilon_r^\nu(k_2)\,\varepsilon_s^{\mu^*}(k_1)\,\varepsilon_r^\sigma(k_2)\,\varepsilon_s^{\rho^*}(k_1)\\ &\sum_{spin}\bar v(p_2)\,\gamma^r p_t\gamma^\mu u(p_1)\,\bar u(p_1)\,\gamma^\sigma p_t\gamma^\rho v(p_2)\\ =& \frac{N^2-1}{2N^2}\cdot\frac{1}{2}\cdot\frac{(eQg)^2}{ut}\,\mathrm{TR}\left[\not{p}_2\gamma_\nu\not{p}_t\gamma_\mu\not{p}_1\gamma^\nu\not{p}_u\gamma^\mu\right]. \qquad (5.31)\end{aligned}$$

The trace in (5.31) can be calculated as

$$\begin{aligned}\mathrm{TR}\left[\not{p}_2\gamma_\nu\not{p}_t\gamma_\mu\not{p}_1\gamma^\nu\not{p}_u\gamma^\mu\right] &= p_2^\alpha p_t^\beta p_1^\sigma p_u^\rho\,\mathrm{TR}\left[\gamma_\alpha\gamma_\nu\gamma_\beta\gamma_\mu\gamma_\sigma\gamma^\nu\gamma_\rho\gamma^\mu\right]\\ &= -2p_2^\alpha p_t^\beta p_1^\sigma p_u^\rho\,\mathrm{TR}\left[\gamma_\alpha\gamma_\sigma\gamma_\mu\gamma_\beta\gamma_\rho\gamma^\mu\right]\\ &= -2p_2^\alpha p_t^\beta p_1^\sigma p_u^\rho\cdot 4g_{\alpha\rho}\cdot 4g_{\alpha\sigma}\\ &= -32(p_tp_u)(p_2p_1) = -32\cdot\frac{1}{4}\cdot s(t+s+u) = -8s(t+s+u).\end{aligned}$$

Now we just have to put all pieces together. Adding up the three single expressions after inserting the calculated traces yields

$$\overline{|M|^2}_{q\bar{q}\to\gamma g} = (eQg)^2 \frac{N^2-1}{N^2}\left(\frac{t^2+u^2+2s(t+s+u)}{tu}\right).$$

5.4 Recap of the Results

To get a better overview, the essential points of the calculation are summarized below. The quark masses were set to $m_{quark} = 0$, which significantly simplifies the calculation. Besides that, we can express the matrix elements in terms of Mandelstam variables. The final matrix elements for unpolarized particles are given in Table 1.

Process	$\overline{\lvert M\rvert^2}$
$q\ g \to q\ \gamma$	$-\frac{(eQg)^2}{N}\left[\frac{u^2+s^2-2t(u+s+t)}{us}\right]$
$\bar{q}\ g \to \bar{q}\ \gamma$	$-\frac{(eQg)^2}{N}\left[\frac{u^2+s^2-2t(u+s+t)}{us}\right]$
$q\ \bar{q} \to g\ \gamma$	$\frac{(eQg)^2(N^2-1)}{N^2}\left[\frac{t^2+u^2-2s(u+s+t)}{tu}\right]$

Table 1: Matrix elements of the contributing processes. The red marked terms are negligible.

For real photons the mass is $m_\gamma = 0$, which leads to the following simplification, that is marked red in Table 1

$$\begin{aligned} u+s+t &= -2p_2k_1 + 2k_1k_2 - 2p_1k_1 = k_1\left(k_2 - p_1 - p_2\right) \\ &= k_1\left(k_2 - k_2 - k_1\right) = -k_1^2 = m_\gamma = 0. \end{aligned} \tag{5.32}$$

6 Kinematics

The last thing we need to do is to determine the kinematics in order to calculate the cross section of action. The goal of this chapter is therefore to put the kinematics into a suitable form to compare the results with the experiment.
The Lorenz invariant phase-space element for two outgoing particles is given by

$$dPS_2 = \frac{1}{(2\pi)^2}\delta^{(4)}\left(p_A + p_B - k_1 - k_2\right)\frac{d^3k_1}{2E_1}\frac{d^3k_2}{2E_2}. \tag{6.1}$$

$\frac{d^3k}{2\pi E}$ denotes the phase-space elements of the single particles and the delta-function four momentum conservation.
The differential cross section is given by the following expression[13]

$$\begin{aligned} d\sigma &= \frac{|M|^2}{F}\cdot dPS_2 \\ &= \frac{|M|^2}{F}\cdot\frac{1}{(2\pi)^2}\cdot\delta^{(4)}\left(p_A + p_B + k_1 + k_2\right)\frac{d^3k_1}{2E_1}\frac{d^3k_2}{2E_2}. \end{aligned} \tag{6.2}$$

As previously discussed, the most beneficial specification of the differential cross section is given by $E_1\frac{d^3\sigma}{dk_1^3}$. Considering this, (6.2) changes into

$$\Rightarrow E_1\frac{d^3\sigma}{dk_1^3} = \frac{1}{F}\cdot|M|^2\cdot\frac{1}{(2\pi)^2}\delta^{(4)}\left(p_A + p_B + k_1 + k_2\right)\frac{d^3k_2}{4E_2}. \tag{6.3}$$

This is the basic equation expressing the differential cross section. To compare this calculation with the experiment, the cross section has to be „translated“ from the parton- to the proton-frame. This is done by integrating over all possible momentum scales x_1, x_2 weighted by the density function, which describes the probability of getting a parton at a certain momentum scale x

$$E_1\frac{d^3\sigma}{dk_1^3} = \sum_{a,b}\int dx_1dx_2\; f_a(x_1)f_b(x_2)\frac{d^3\hat{\sigma}_{a,b}}{dp_1^3}(x_1,x_2). \tag{6.4}$$

It is easy to get confused, which frame we are talking about. For that, we will label parton momenta and energies with 1,2 and proton momenta and energies A,B. The calculation is done exemplarily for two undistinguished flavors a and b.

$$E_1\frac{d^3\sigma}{dk_1^3} = \int dx_1dx_2f(x_1)f(x_2)\frac{1}{(2\pi)^2}\frac{dk_{2,z}}{4E_2}dk_{2,T}^2\;\delta^{(4)}(x_1P_A + x_2P_B - k_1 - k_2)\frac{1}{F}|\bar{M}|^2. \tag{6.5}$$

In order to get the cross section into an expression, which we can evaluate numerically, we have to eliminate the delta function. $\delta^{(4)}$ can be written as

$$\delta^{(4)}(\ldots) = \delta(x_1E_A + x_2E_B - E_1 - E_2)\delta^{(2)}(\vec{k}_{1,T} + \vec{k}_{2,T})\delta(x_1p_{A,z} + x_2p_{B,z} - k_{1,z} - k_{2,z}). \tag{6.6}$$

[13] This was described in section 4.

For high energy collisions (here $\sqrt{s} = 22.985$ GeV) the Proton-masses ($m_P \approx 1$ GeV) can be neglected. This does not seem to be true at the first look. However, the Proton momentum is given by

$$p = \sqrt{E^2 + m^2} = \sqrt{11.499^2 + 1^2}\ \text{GeV} \approx \sqrt{11.499^2}\ \text{GeV}. \tag{6.7}$$

Because the energy and mass are squared, the error is below 1%. This simplification leads to

$$m_A = m_B \approx 0 \ \Rightarrow\ E := E_A = E_B \approx P_{A,z} = -P_{B,z} \tag{6.8}$$

$$\sqrt{s} \approx 2E. \tag{6.9}$$

Carrying out the integral of (6.5), utilizing the delta function (6.6) yields

$$dx_1\delta(x_1E + x_2E - E_1 - E_2) = dx_1\frac{1}{E_A}\delta\left(x_1 + \frac{x_2E\_E_1 - E_2}{E}\right) \tag{6.10}$$

$$\Rightarrow x_1 = \frac{E_1 + E_2 - x_2E}{E}. \tag{6.11}$$

The same can be done for dx_2, inserting (6.10) in the second step

$$dx_2\delta\left(x_1E - x_2E - k_{1,z} - k_{2,z}\right) = dx_2\frac{1}{E}\delta\left(x_2 - \frac{E_1 + E_2 - k_{1,z} - k_{2,z}}{2E}\right). \tag{6.12}$$

This also leads to a restriction for x_2

$$\Rightarrow x_2 = \frac{E_1 + E_2 - k_{1,z} - k_{2,z}}{\sqrt{s}}. \tag{6.13}$$

Inserting (6.13) into (6.11) leads to the final condition for x_1

$$\Rightarrow x_1 = \frac{E_1 + E_2 + k_{1,z} + k_{2,z}}{\sqrt{s}}. \tag{6.14}$$

The last $\delta^{(2)}$ just pictures conservation of transversive momentum

$$dk_T^2\ \delta^{(2)}(\vec{k}_{1,T} + \vec{k}_{2,T})\ \Rightarrow\ \vec{k}_{1,T} = -\vec{k}_{2,T}\ \text{ or rather }\ k_T := k_{1,T} = k_{2,T}. \tag{6.15}$$

So the cross section simplifies to the following expression [14]

$$E_1\frac{d^3\sigma}{dk_1^3} = \int \frac{dk_{2,z}}{E_{2,}} f_a\left(x_1\right) f_b\left(x_2\right) |\overline{M}|^2 \frac{1}{16\pi^2}\frac{1}{F}\frac{1}{2E_AE_B}. \tag{6.16}$$

The factor $\frac{1}{2E_AE_B}$ is caused by the integration in (6.10) and (6.12). The flux F is $2\hat{s} = 2s \cdot x_1x_2$, i.e. depends on x_1 and x_2.

[14] We only have to keep in mind that x_1 and x_2 depend on $k_{2,z}$.

The four momentum vector k^μ can be written in terms of rapidity y

$$k^\mu = \left(E_T \cosh(y), k_x, k_y, E_T \sinh(y)\right) \ , E_T = \sqrt{k_T^2 + m^2} \approx k_T \tag{6.17}$$

$$y = \frac{1}{2} \ln \frac{E + k_z}{E - k_z}. \tag{6.18}$$

Finally one can make the substitution

$$\frac{dk_{2,z}}{dy_2} = E_T \cosh y_2 = E_2 \ \Rightarrow \ \frac{dk_{2,z}}{E_2} = dy_2. \tag{6.19}$$

To calculate the integral, one has to consider how x_1 and x_2 depend on y_2. Inserting the energy- and z-component (6.17) into (6.14) and (6.13) yields

$$x_{1/2} = \frac{k_T}{\sqrt{s}} \left(\cosh(y_1) + \cosh(y_2) \pm \sinh(y_1) \pm \sinh(y_2)\right) \tag{6.20}$$

$$x_1 = \frac{k_T}{\sqrt{s}} \left(e^{y_1} + e^{y_2}\right) \quad \text{and} \quad x_2 = \frac{k_T}{\sqrt{s}} \left(e^{-y_1} + e^{-y_2}\right). \tag{6.21}$$

7 Numerical Calculations

For the numerical calculation and subsequent comparison with experimental data, the rapidity y_1 is set to 0, leading to x_1 and x_2.

$$x_1 = \frac{k_T}{\sqrt{s}}\left(1 + e^{y_2}\right), \quad x_2 = \frac{k_T}{\sqrt{s}}\left(1 + e^{-y_2}\right). \tag{7.1}$$

We can estimate the integration limits by considering the restrictions made for x_1 and x_2

$$0 < x < 1. \tag{7.2}$$

This applies independently to both variables x_1, x_2 and restricts y_2 to the interval

$$-\ln\left(\frac{\sqrt{s}}{k_T} - 1\right) < y_2 < \ln\left(\frac{\sqrt{s}}{k_T} - 1\right). \tag{7.3}$$

This can simply be checked by observing the upper and lower bounds for x_1 and x_2. For values below the lower bound, x_2 gets larger than 1. The upper bound of y_2 is not restricted by x_2, since the exponential term in (7.1) just decreases for large y_2. The same connection applies to the lower bound and x_1 because it depends of $x_1(y_2) = x_2(-y_2)$.

Needed constants for the cross section are the electromagnetic (and strong) coupling constant e (g). Since natural units are used the coupling constants yield

$$e = \sqrt{4\pi\alpha} \qquad \alpha \approx \frac{1}{137} \tag{7.4}$$

$$g = \sqrt{4\pi\alpha_s}. \tag{7.5}$$

For the numerical calculations, momenta and energies are initialized in GeV. Transforming this into nb/GeV^2 is done by simply multiplying with the factor 0.382 [4]. The electromagnetic coupling can be assumed to be constant, whereas α_s has to be calculated according to section 2.

7.1 Experimental Setup

In the WA70 experiment at CERN SPS, cross sections of processes in π^--p- , π^+-p- and p-p-collisions were measured. The made calculations apply to the direct photon production in proton-proton collisions with a γ-rapidity of $\eta_\gamma = 0$. Numerical calculations are made with Python, using the parton package from LHAPDF[2].

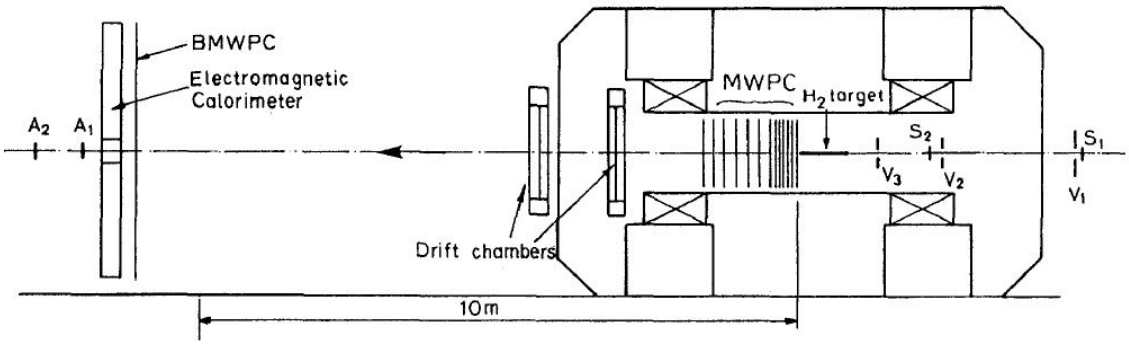

Figure 7: Schematic depiction of the experimental setup. [8]

As shown in Figure 7, the proton-proton-collisions are performed on a 1 m long fixed hydrogen (H_2-target). The outgoing photons are detected in the electromagnetic calorimeter at a distance if 10.9 m.[15]
The previous calculations are made in the cms-system. To compare the experimental data to the calculations, the cross sections can be used. As mentioned in section 4, the cross section is constructed to be invariant under boosts. Since $E\frac{d^3}{dp^3}$ is Lorenz invariant as well [16], the calculations are directly comparable to WA70 data.
The used data is chosen for a rapidity of $\eta_\gamma = 0$. The data [8] is measured in x_T-bins

$$x_T = \frac{2p_{T,cm}}{\sqrt{s}}. \tag{7.6}$$

In order to get data corresponding to $\eta_\gamma = 0$, we just have apply $x_T = 0$:

$$\eta_\gamma = \frac{1}{2}\ln\left(\frac{|\mathbf{p}| - p_T}{|\mathbf{p}| + p_T}\right) \overset{p_T \to 0}{=} \frac{1}{2}\ln(1) = 0. \tag{7.7}$$

Finally the used bin reads

$$x_T \in [0.15, 0.15]\,. \tag{7.8}$$

[15] For a more detailed description see [8].
[16] This is shown in subsection A.5.

8 Results And Comparison To WA70 Data

The results are calculated based on the previous calculations and definitions. The energy scale Q is chosen in dependence on the transverse photon momentum k_T. This choice affects the strong coupling constant and the PDFs, which both depend on Q. In order to get an uncertainty for this scale dependency, the differential cross section can be calculated for $Q = k_T/3$ and $Q = k_T$, which is done in Figure 8. The dyed area between the predictions represents the uncertainty.

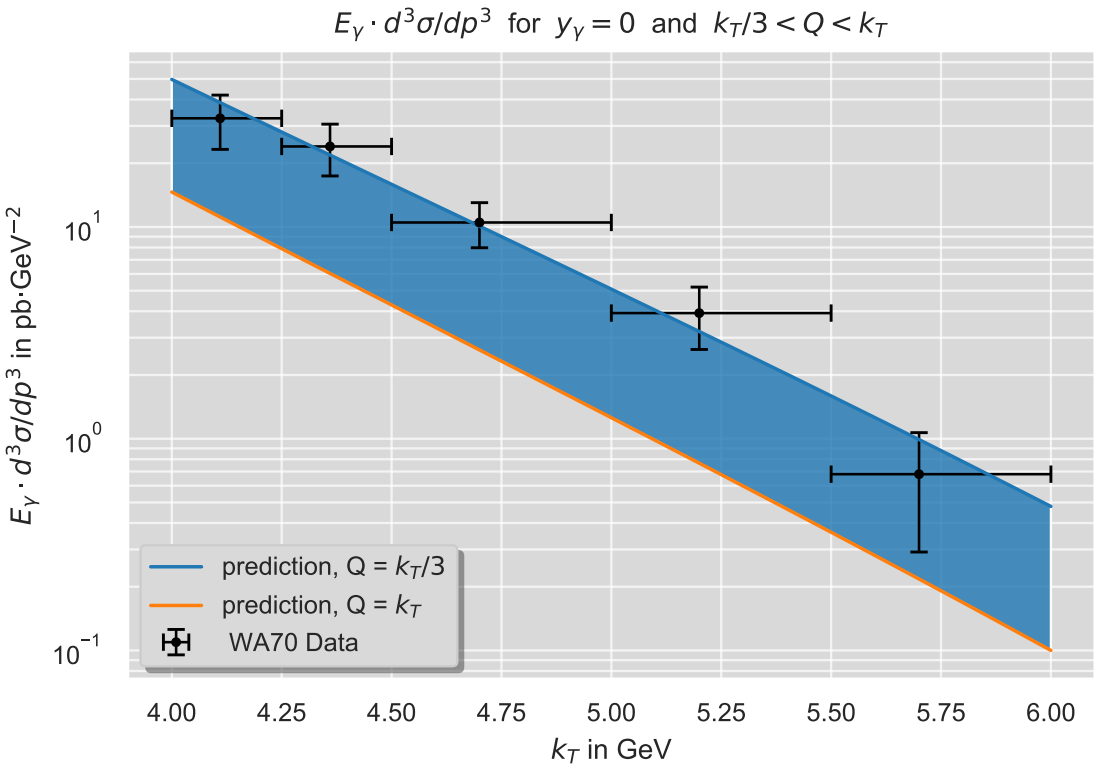

Figure 8: Differential cross section as a function of the transversive photon momentum k_T. The data is taken from the WA70 collaboration [8] at $\sqrt{s} = 22.957$GeV. The uncertainty of the theoretical prediction includes scale errors.

The k_T errors represent the bin size. The total error of $\frac{d^3\sigma}{dp^3}$ data contains systematic and statistical errors, which have been added quadratically

$$u_{total} = \sqrt{u_{stat}^2 + u_{syst}^2}. \tag{8.1}$$

The prediction matches the data within the uncertainties. However, the scale error, induced by the strong coupling constant and the PDFs, is too large to make a precise prediction. The strong coupling constant and PDF vary widely on low momentum scales. Hence, the low transverse momentum leads to a particularly high uncertainty since we choose Q as a function of k_T. A leading order calculation is therefore insufficient.

Second, we need to consider the error of the parton distribution functions. The PDF sets, described in section 7, are used. The propagation of the PDF error is calculated according to (8.2) [7]

$$u(X) = \frac{1}{2}\sqrt{\sum_{i=1}^{26}\left(X(f_i^+) - X(f_i^-)\right)^2}. \tag{8.2}$$

The CT18 PDF sets contain 58 members f_k, of which even members represent $f_{2k} = f_k^+$ and odd members $f_{2k+1} = f_k^-$.

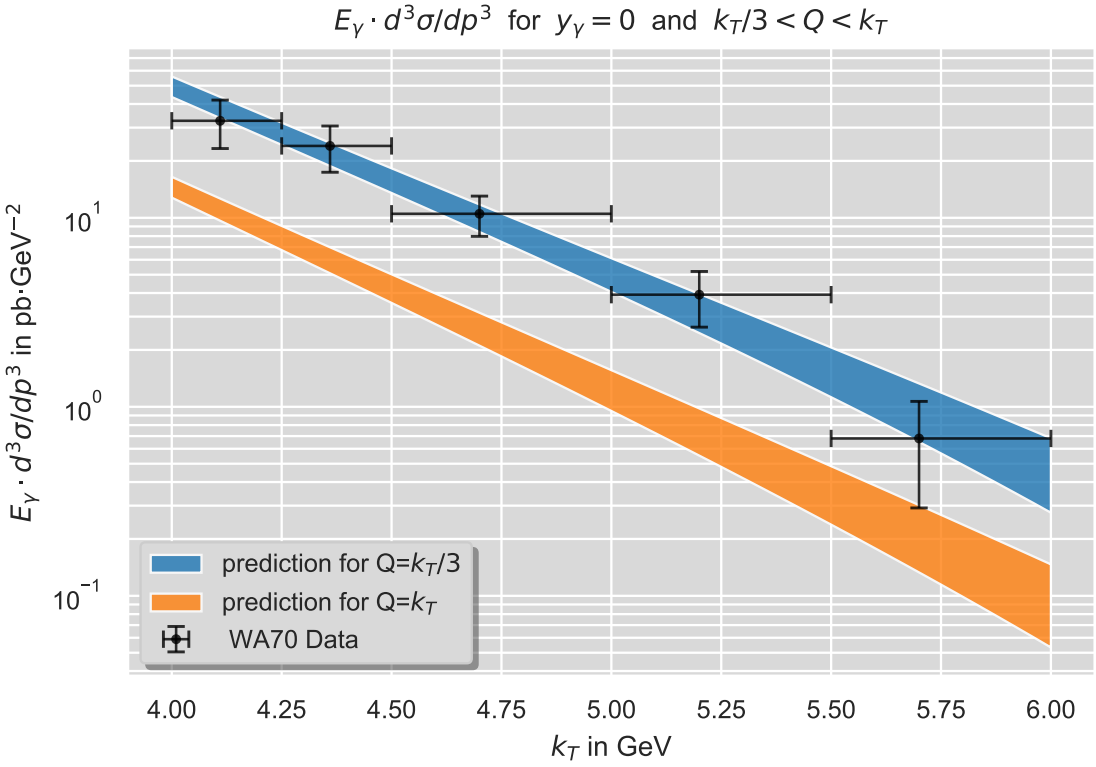

Figure 9: Differential cross section as a function of the transverse photon momentum k_T. The data is taken from from the WA70 collaboration [8] at $\sqrt{s} = 22.957$GeV. The uncertainty of the theoretical prediction includes scale errors.

For $Q = k_T/3$, the prediction matches the data within the uncertainties. The PDF error is mainly induced by the gluon PDF, which contains high uncertainties for high x.

For the total error we can assume an energy scale $Q_0 = k_T/2$. The upper and lower differences to $Q_u = k_T/3$ and $Q_l = k_T$ correspond to the uncertainty (see Figure 8). We can compute the PDF error separately and add both uncertainties quadratically.

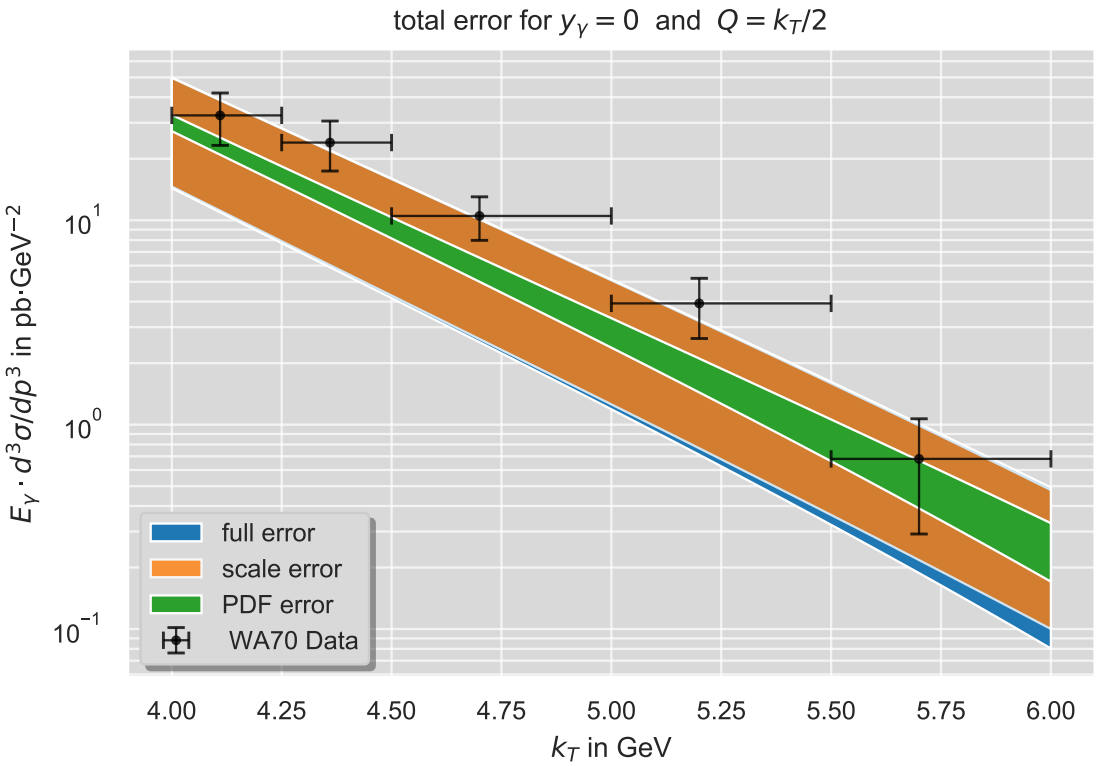

Figure 10: Differential cross section as a function of the transverse photon momentum k_T. The data is taken from from the WA70 collaboration [8] at $\sqrt{s} = 22.957$GeV. The uncertainty of the theoretical prediction includes scale and PDF errors.

The total error shown in the Figure 10 mainly depends on the scale error. Thus, due to the previously discussed effects, scale dependence dominates the uncertainty.

To estimate the relative PDF error, we choose a scale of $Q = k_T/3$. The relative PDF error is given by the ratio of the error (8.2) and the differential cross section. In order to obtain a relative scale error, we can calculate the ratio of the mean value and $Q = k_T/3, Q = k_T$. The uncertainty is calculated according to

$$u_{\text{scale}} = \frac{d^3\sigma_{\text{mean}}}{d^3\sigma_{Q=k_T/3} - d^3\sigma_{\text{mean}}}. \tag{8.3}$$

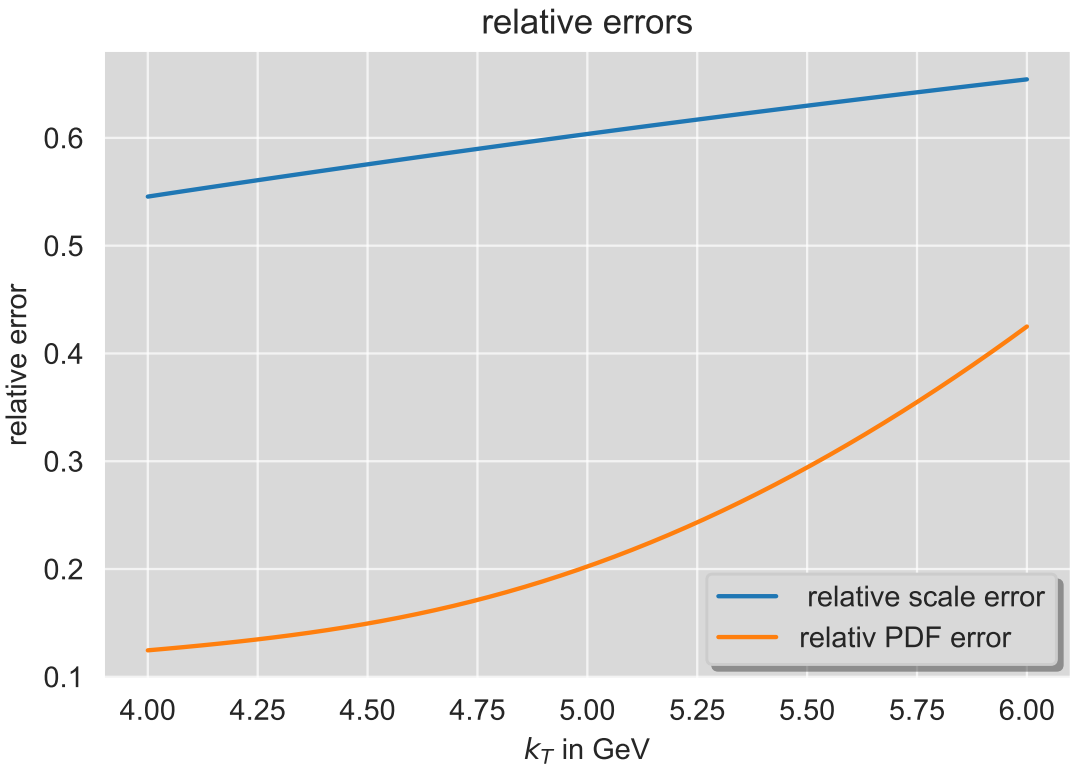

Figure 11: Relative errors in dependence of k_T in GeV. The PDF error is obtainen according to (8.3). For the relative PDF error, an energy scale of $Q = k_T/3$ is used.

The relative scale uncertainty is weakly dependent on k_T and is about 60%. In contrast, the relative scale error is increasing with k_T, up to 43%.

For the leading order calculation, we considered three processes. The ratio of each process share is shown in Figure 12.

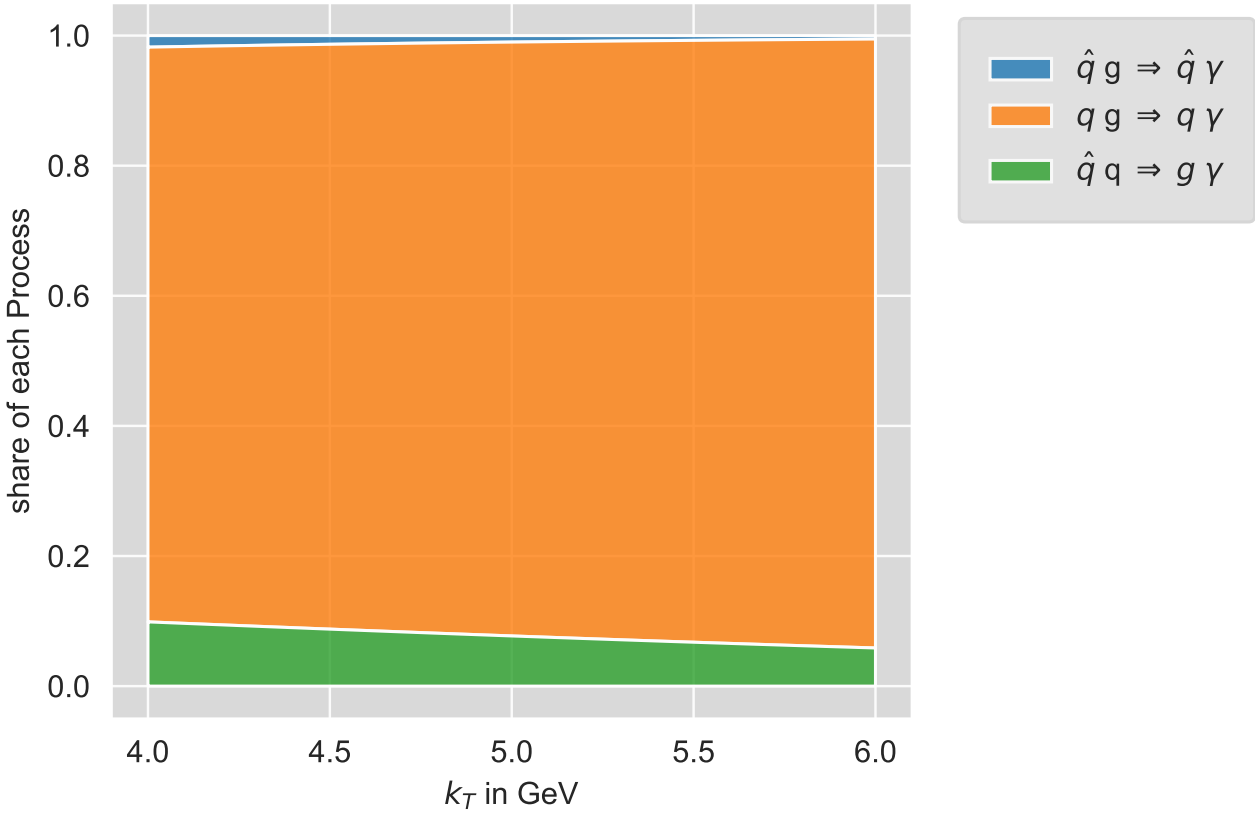

Figure 12: Fraction of the direct photon prodution as a function of the transverse photon momentum k_T. For the calculation an energy scale of $Q = k_T/3$ is chosen.

As shown in Figure 12, the ratio of *quark-antiquark annihilation* starts with a share of 9.8% ($k_T = 4$ GeV) and decreases with increasing k_T to 5.8% ($k_T = 6$ Gev). The *hard compton scattering* accounts for the largest share, 88% at 4 GeV and 93% at 6 GeV. Since antiquarks are unlikely to be found at low energe scales, the share of *anti compton scattering* is very weak, i.e. only accounts for 1.7% at 4 GeV. The same argument applies to quark antiquark annihilation.

9 Conclusion

Under consideration of *uncertainties*, the theoretical prediction *matches the WA70 data*. This yields for scale errors (see Figure 8) as for PDF-errors (see Figure 9). However, the total errors are too large to make a precise prediction.
The *scale errors* are induced by the dependence of the *parton distribution functions* at low energy scales and the *strong coupling constant*. We could simply reduce these errors by using higher energies in the experiment. This would lead to a smaller variation of the PDF, as shown in Figure 3 and the strong coupling constant (see Figure 1), since it becomes infinitesimal for small energy scales because of confinement. Furthermore, the *PDF error* is mainly generated by the high uncertainty of the *gluon PDF* at large momentum fractions ($x_{gluon} \to 1$).
A determination of the *process shares* shows that the cross section is primarily determined by the hard Compton scattering with a ratio of 88%. Quark antiquark annihilation makes up a ratio of 10%, where anti Compton scattering has a vanishing small process ratio of 2%.
In conclusion, it can be stated that the *large errors* (over 60% of the cross section) do not allow a meaningful prediction. *The calculation at tree level is therefore insufficient.*

A Relations

A.1 Completeness Relation and Polarization Sum

The completeness relations for u- and v-spinors are

$$\sum_{s=1,2} u^{(s)}(p)\bar{u}^{(s)}(p) = \not{p} + m \tag{A.1}$$

$$\sum_{s=1,2} v^{(s)}(p)\bar{v}^{(s)}(p) = \not{p} - m. \tag{A.2}$$

The polarization sum for massles particles is

$$\sum_{T} \varepsilon_{\mu}^{T*}\varepsilon_{\nu}^{T} = -g_{\mu\nu}. \tag{A.3}$$

A.2 SU(N) Relations

The generators of SU(N) satisfy the following commutator relation.

$$\left[T^a, T^b\right] = if^{abc}T^c. \tag{A.4}$$

In the fundametial representation, the sum over the product of two operators is given by

$$\sum_{a,k} (T_F^a)_{ik}\,(T_F^a)_{kj} = C_F\delta_{ij}\,, \qquad C_F = \frac{N^2-1}{2N}. \tag{A.5}$$

The trace of the SU(N) generators yields

$$\sum_{a,k,i} (T_F^a)_{ik}\,(T_F^a)_{ki} = \sum_{i} \frac{N^2-1}{2N}\delta_{ii} = \frac{N^2-1}{2}. \tag{A.6}$$

The averaging-factors Z for ingoing gluons and quarks are

$$\begin{aligned} Z_{quark} &= \frac{1}{N} \\ Z_{gluon} &= \frac{1}{N^2-1}. \end{aligned} \tag{A.7}$$

A.3 Trace Theorems

Used trace theorems are given by

$$\mathrm{TR}\left[\gamma^\mu\gamma^\nu\gamma^\rho...\right] = 0 \quad \forall \text{ odd numbers of } \gamma\text{-Matrices} \tag{A.8}$$

$$\mathrm{TR}\left[\gamma^\mu\gamma^\nu\right] = 4\eta^{\mu\nu} \tag{A.9}$$

$$\mathrm{TR}\left[\gamma^\mu\gamma^\nu\gamma^\rho\gamma^\sigma\right] = 4(\eta^{\mu\nu}\eta^{\rho\sigma} - \eta^{\mu\rho}\eta^{\nu\sigma} + \eta^{\mu\sigma}\eta^{\nu\rho}) \tag{A.10}$$

$$\mathrm{TR}\left[\gamma^5\right] = \mathrm{Tr}\left[\gamma^\mu\gamma^\nu\gamma^5\right] = 0 \tag{A.11}$$

$$\mathrm{TR}\left[\gamma^\mu\gamma^\nu\gamma^\rho\gamma^\sigma\gamma^5\right] = 4i\varepsilon^{\mu\nu\rho\sigma} \tag{A.12}$$

$$\mathrm{TR}\left[\gamma^{\mu_1}\dots\gamma^{\mu_N}\right] = \mathrm{TR}\left[\gamma^{\mu_N}\dots\gamma^{\mu_1}\right]. \tag{A.13}$$

A.4 Feynman Rules

To calculate the corresponding matrix elements for the Feynman diagramms, the following Feynman rules are used.

Calculation of the vertices yields:

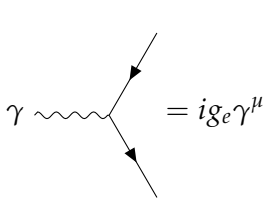

$$= ig_e\gamma^\mu$$

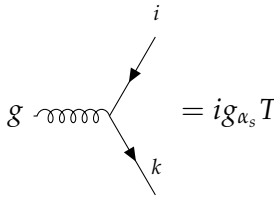

$$= ig_{\alpha_s} T^a_{ik}\gamma^\mu \tag{A.14}$$

The fermion propagator is given by:

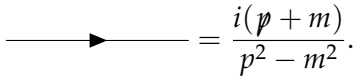

$$= \frac{i(\not{p} + m)}{p^2 - m^2}. \tag{A.15}$$

Outgoing fermion lines are given by:

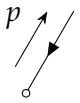

$$= v(p)$$

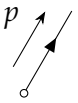

$$= \bar{u}(p) \tag{A.16}$$

Ingoing fermion lines are given by:

$$= \bar{v}(p)$$

$$= u(p) \tag{A.17}$$

In- and outgoing boson lines are given by:

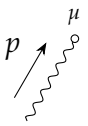

$$= \varepsilon^\mu_r(p)$$

$$= \varepsilon^{\mu *}_r(p) \tag{A.18}$$

A.5 Lorenz Invariants

$$\begin{aligned} dp^4\delta\left(p^2 - m^2\right) &= d^2\vec{p}\, dp_0\delta\left(p_0^2 - \vec{p}^2 - m^2\right) = \\ &= d^3\vec{p}\, \frac{dp_0}{2p_0}\, \delta\left(p_0 - \vec{p}^2 - m^2\right) = \\ &= d^3\vec{p}\, \frac{1}{2E}. \end{aligned} \tag{A.19}$$

B Gluon Couplings

B.1 3 Gluon Coupling

To outline the calculation of the 3 gluon coupling, it is sufficient to just calculate the first term [17]

$$\mathscr{L}_{3\text{ gluon}} = -ig\left[\mathcal{A}^\mu, \mathcal{A}^\nu\right]\left(\partial_\nu \mathcal{A}_\mu - \partial_\mu \mathcal{A}_\nu\right). \tag{B.1}$$

Applying the trace we neglected yields

$$\begin{aligned}\mathscr{L}_{3\text{ gluon}} &= -igA_a^\mu A_b^\nu \left(\partial_\nu A_\mu^c - \partial_\mu A_\nu^c\right) \mathrm{TR}\left[T_a T_b T_c - T_b T_a T_c\right] \\ &= -igA_a^\mu A_b^\nu \left(\partial_\nu A_\mu^c - \partial_\mu A_\nu^c\right) \frac{i}{2} f_{abc}. \end{aligned} \tag{B.2}$$

The momentum can be written as $i\partial_\nu A^\nu = p_\nu A^\nu$. Applying this, yields

$$\mathscr{L}_{3\text{ gluon}} = -igA_a^\mu A_b^\nu i\left(-i\partial_\nu A_c^\lambda g_{\mu\lambda} + i\partial_\mu A_c^\lambda g_{\nu\lambda}\right)\frac{i}{2} f_{abc} \tag{B.3}$$

$$= \frac{ig}{2} f_{abc}\left(g_{\nu\lambda} p_\mu - g_{\mu\lambda} p_\nu\right) A_a^\mu A_b^\nu A_c^\lambda. \tag{B.4}$$

Adding the second part of the 3 gluon interaction term eliminates the factor $1/2$.

B.2 4 Gluon Coupling

$$\begin{aligned}\mathscr{L}_{4\text{ gluon}} &= -g^2\left[\mathcal{A}^\mu, \mathcal{A}^\nu\right]\left[\mathcal{A}_\nu, \mathcal{A}_\mu\right] \\ &= -g^2 A_a^\mu A_b^\nu \left[T_a, T_b\right] A_\nu^d A_\mu^e \left[T_d, T_e\right] \\ &= g^2 A_a^\mu A_b^\nu A_\mu^d A_\nu^e \; f_{abc} f_{def} \; T_c T_f. \end{aligned}$$

As mentioned in section 1, we have still to consider the trace. This affects only the SU(3)-generators

$$\mathrm{TR}\left[T_c T_f\right] = \delta_{cf}. \tag{B.5}$$

Keeping in mind, that we still have to consider all permutations the coupling term yields

$$\mathscr{L}_{4\text{ gluon}} = g^2 \; f_{abc} f_{def} \; g^{\nu\rho} g^{\mu\sigma} A_a^\mu A_b^\nu A_d^\rho A_e^\sigma. \tag{B.6}$$

To finally receive the correct expression, outlined in section 1, we have to consider all permutations of the fields and add them together and multiply with the factor $-1/4$, which was neglected in section 1 and i. The calculation shown here is intended to illustrate the form of the coupling in the first instance.

[17] The calculation of the second term is identical.

References

[1] S. J. Brodsky A. Deur and G. F. de Téramond. *The QCD Running Coupling*. URL: http://dx.doi.org/10.1016/j.ppnp.2016.04.003. (Stand Juni 2018, zugegriffen: 11.07.2021).

[2] Andy Buckley et al. "LHAPDF6: parton density access in the LHC precision era". In: *The European Physical Journal C* 75.3 (Mar. 2015). ISSN: 1434-6052. DOI: 10.1140/epjc/s10052-015-3318-8. URL: http://dx.doi.org/10.1140/epjc/s10052-015-3318-8.

[3] David dEnterria. *αs status and perspectives (2018)*. URL: https://arxiv.org/abs/1604.08082. (Stand Juni 2018, zugegriffen: 12.07.2021).

[4] Francis Halzen and Alan Martin. *Quarks & Leptons: An introductory course in modern particle physics*. New York, USA: John Wiley & Sons, 1984.

[5] TAO HAN. "COLLIDER PHENOMENOLOGY: BASIC KNOWLEDGE AND TECHNIQUES". In: *Physics In D 4 Tasi 2004* (July 2006). DOI: 10.1142/9789812773579_0008. URL: http://dx.doi.org/10.1142/9789812773579_0008.

[6] Tie-Jiun Hou et al. "New CTEQ global analysis of quantum chromodynamics with high-precision data from the LHC". In: *Physical Review D* 103.1 (Jan. 2021). ISSN: 2470-0029. DOI: 10.1103/physrevd.103.014013. URL: http://dx.doi.org/10.1103/PhysRevD.103.014013.

[7] K. Kova k et al. "nCTEQ15: Global analysis of nuclear parton distributions with uncertainties in the CTEQ framework". In: *Phys. Rev. D* 93 (8 Apr. 2016), p. 085037. DOI: 10.1103/PhysRevD.93.085037. URL: https://link.aps.org/doi/10.1103/PhysRevD.93.085037.

[8] *Production of High Transverse Momentum Prompt Photons and Neutral Pions in Proton Proton Interactions at 280-GeV/c*. Data Collection. 1988. DOI: 10.17182/hepdata.15647. URL: https://doi.org/10.17182/hepdata.15647.

[9] Matthew D. Schwartz. *Quantum Field Theory and the Standard Model*. Cambridge University Press, Mar. 2014. ISBN: 978-1-107-03473-0, 978-1-107-03473-0.

[10] Jakob Schwichtenberg. *Physics from Symmetry*. Undergraduate Lecture Notes in Physics. Cham: Springer International Publishing, 2018. ISBN: 978-3-319-66630-3, 978-3-319-66631-0. DOI: 10.1007/978-3-319-66631-0.

Declaration of Academic Integrity

I hereby confirm that this thesis on *Direct Photon Production in Proton-Proton-Collisions* is solely my own work and that I have used no sources or aids other than the ones stated. All passages in my thesis for which other sources, including electronic media, have been used, be it direct quotes or content references, have been acknowledged as such and the sources cited.

_____
(date and signature of student)

I agree to have my thesis checked in order to rule out potential similarities with other works and to have my thesis stored in a database for this purpose.

_____
(date and signature of student)